System in Package (SiP) with Embedded Antenna

HAMED BAHARIPANBEHCHOULEH
MASTER´S THESIS
DEPARTMENT OF ELECTRICAL AND INFORMATION TECHNOLOGY
FACULTY OF ENGINEERING | LTH | LUND UNIVERSITY

System in Package (SiP) with Embedded Antenna

Hamed Baharipanbehchouleh
ha4808ba-s@student.lu.se

Department of Electrical and Information Technology
Lund University

Academic Supervisor: Baktash Behmanesh
Ph.D., Assistant Professor, EIT LTH

Supervisor: Markus Wejrot
u-blox AB

Examiner: Pietro Andreani
Ph.D., Senior Lecturer, EIT LTH

May 21, 2024

LUND UNIVERSITY

Abstract

System in Package (SiP) is often used in wireless technologies where different active and passive components can be integrated under the same substrate, resulting in smaller devices and lower costs. The design of the embedded antennas in system in package is a challenge from various points of view. Since system in packages are often used when a small module is needed, and as the size of the module decreases, the size of the antenna embedded in the SiP should also become smaller, making it complicated to design an antenna with high performance.

The aim of the thesis is to design a very small antenna with a size of 3×10 mm, covering the frequency range from 5.15 to 7.125 GHz, with high performance in terms of return loss, radiation efficiency, peak gain, radiation pattern and other important parameters. The antenna is designed on a 13.4×10.6 mm SiP module mounted on a 30×50 mm carrier board. The performance of the antenna is also investigated at different locations on the carrier board. It is worth mentioning that the components on the module are covered by a metal shield that can affect the performance of the antenna, which was taken into the account during the design. The work included literature studies, design and simulations of an antenna model with acceptable performance and measurements of antenna prototypes. Ansys HFSS, the high-frequency structure simulator, was used for the design and simulation. In the next step, the design was created in Cadence Allegro to be prepared for manufacturing. ROHDE & SCHWARZ ZNB 20 Vector Network Analyzer and the u-blox anechoic chamber were used for the prototype measurements. As a result of this thesis, two printed monopole antennas with a size of 3 ×10 mm were designed and simulated, both of which showed acceptable performance to cover the frequency bandwidth of 5 to 7 GHz in the simulation. The measurements of the prototype were also carried out for some parameters. The focus of this work was on the design of the antenna on a carrier board with FR-4 dielectric substrate and a thickness of 1.6 mm. The antennas were fabricated on a substrate with a total thickness of 0.8 mm (0.4 mm for the module and 0.4 mm for the carrier board) in order to keep the thickness of the module and the carrier board the same for cost reasons. It is worth noting that the behavior of the antennas at this specific thickness was also investigated in this degree project.

Acknowledgments

I would like to take this opportunity to first thank **Peter Karlsson** for supporting me with sharing his profound knowledge throughout this thesis. I am deeply grateful to **Markus Wejrot**, my industrial supervisor, for his guidance, valuable feedback and advice that enabled me to progress and complete the project. I am truly thankful to my academic supervisor, **Baktash Behmanesh** for giving me precious suggestions and guidance in a very professional manner throughout the project.

I would also like to thank **Brian Curran** and **Olof Viklund** for their support and sharing their valuable experience and expertise that enabled me to complete the project at the higher level.

I am sincerely grateful to the other employees of u-blox: **Hozaifa Abdelgadir**, **Aneeb Sohail**, **Yaqin Chen** and **Hakan Ekfors** for their cooperation and collaboration throughout the project.

I would also like to take this opportunity to thank my family for their great support during my Master's studies. My special thanks go to my wife **Narges**, who always has my back and gives me great encouragement.

Popular Science Summary

Nowadays, compact and high performance devices play an important role in the world of wireless technologies. An important innovation in this area is System in Package (SiP), in which multiple silicon components (chips) are integrated into a single package together with other passive components such as capacitors, inductors, antennas, etc. SiP has a wide range of applications nowadays, it can be used in smartphones, wearables and Internet of Things (IoT) modules and is also used for devices such as power amplifier modules, Wi-Fi and Bluetooth modules.

On the other hand, antennas are the technology that plays a crucial role in today's age of information explosion. Antennas are found in all kinds of wireless devices and can connect millions of users wirelessly every day. Antennas can also be embedded as passive components in SiP. The embedded antennas are usually placed at the edge of the module to receive and transmit the electromagnetic waves and are connected to an AC source inside the SiP module. When the antenna acts as a receiver, it converts the electromagnetic waves into an electrical signal and when it acts as a transmitter, it converts the electrical signal into electromagnetic waves. Since the components in the package are very close to each other to form a small module, the embedded antenna is exposed to the proximity of other components, which can affect the performance of the antenna. There are other factors that need to be considered when designing the antenna, such as the position of the antenna in the SiP module and its location in relation to the ground plane, as well as the way the module is placed on the carrier board can be mentioned as factors that can influence the performance of the antenna and should be considered by the designer.

The aim of this master thesis is to create a simulation model of a SiP with embedded antenna, focusing on performance and size. The main focus is on the Wi-Fi bands 5-7 GHz. The design is simulated to create a feasible antenna design and optimize the design to meet the specifications such as bandwidth, radiation characteristics, efficiency, peak gain, return loss, etc. At the end of the project, the design that fulfils the target data for the simulation model was achieved. It is worth mentioning that the final simulated antennas were manufactured and the measurement of the antenna prototypes was carried out to study the behavior of the antenna in the real world. As a final result of the project, two different antennas were achieved that were able to fulfill most of the simulation targets and also showed acceptable performance for some of the parameters measured in the prototype.

Table of Contents

List of Figures

List of Tables

List of Abbreviations

SiP System in Package

IoT Internet of Things

2D Two-dimensional

3D Three-dimensional

PCB Printed Circuit Board

dB Decibel

dBi Decibel Relative to Isotropic

EMC Electromagnetic Compatibility

VSWR Voltage Standing Wave Ratio

Q Quality Factor

RF Radio Frequency

HFSS High-frequency Structure Simulator

FR-4 Glass-reinforced Epoxy Laminate Material

S11 Scattering Coefficient

S12 Scattering Coefficient

UWB Ultra Wide Band

Z Complex Impedance

R Resistance

X Imaginary Reactance

GCPW Grounded Coplaner waveguide

PRMA Printed Rectangular Monopole Antenna

PSMA Printed Square Monopole Antenna

1. Introduction

Chapter 1

The demand for smart products and wireless devices with compact size and high performance is growing these days. In addition, the market demands the products that can be brought to market quickly, and design flexibility is desired by designers. System in package is the technology that can overcome these challenges by focusing on creating a system that can be considered as a component instead of creating a single component. Smaller and lighter products with lower costs and a higher degree of system integration can be the benefits of system in package technology.

The development of the Internet of Things (IoT), has made the compact wireless modules an indispensable components in the modern life and their antennas are gradually evolving from external devices to integrated devices [1]. There are different types of antennas, each used for specific purposes and applications in wireless communication devices such as Wi-Fi routers, radio and television broadcasting, satellite communications and microwave links, radar systems, etc. Great efforts have been made to find the right antenna geometries, to satisfy the requirements of wireless communication systems [2] [3] [4]. Embedded antennas in System in Package are useful in some applications such as Wi-Fi and Bluetooth modules and are usually very small. The behavior of an antenna is judged by parameters such as bandwidth, radiation pattern, radiation efficiency, gain, reflection coefficient, etc., and these parameters depend on the structure and topology of the antenna.

Designing embedded antennas with small size would be challenging from various points of view, and their vicinity to other components can also lead to undesirable behavior of the antenna. For example, metal shields, which are commonly used for electromagnetic compatibility (EMC) reasons, can affect the parameters of the antenna if they are close to the antenna. In practice, SiP modules are usually placed on a larger carrier board, which can present a new challenge when designing the antenna on a SiP module, as the position of the module on the carrier board can also influence the behavior of the antenna. The layout of the ground plane can be considered to be another factor that affects the performance of the antenna. The direction of the radiated waves is also an important factor that depends on the specification of the design.

1.1. Project Specification

The aim of this master thesis was to design an antenna embedded in a system in package. The design specifications, as shown in Table 1.1, apply to case where designed antenna on the module, is placed on the center of the smaller side of a carrier board with size of 30 × 50 mm. The designed antenna hade to fulfill the requirements of the simulation.

In addition, the measurements of the prototype of the designed antenna had to be carried out in order find out how the antenna behaves in the real environment.

Table 1.1: Project Specification

Antenna type	Monopole antenna
Frequency Band	5.150 – 5.850 GHz, 5.925 – 7.125 GHz
Return loss	< -4.5 dB (5.150 – 5.850 GHz) , < -4 dB (5.925 – 7.125 GHz)
Efficiency	> 65% (5.150 – 5.850 GHz) , > 60% (5.925 – 7.125 GHz)
Peak Gain	1-3 dBi
Radiation Pattern	Omni-directional
Physical size	3 × 10 mm
Substrate Material	FR-4 , 2 mm total thickness, 4.4 relative permittivity

1.2. Thesis Organization

The report is structured as follows:

Chapter 2: Background of antennas, different types of antennas, the concept of different parameters of antennas

Chapter 3: Various Printed Circuit Board (PCB) characteristics and their effects on the antennas, the ground plane and its influence on the antenna

Chapter 4: Design of the proposed antenna, simulation results, comparison of the different scenarios

Chapter 5: The result of the measurement of the prototypes, comparison with the simulation results

Chapter 6: Conclusion of the project

Chapter 7: Future work considering the designed antenna

As illustrated in Figure 1.1, the green area without shielding is the antenna area.

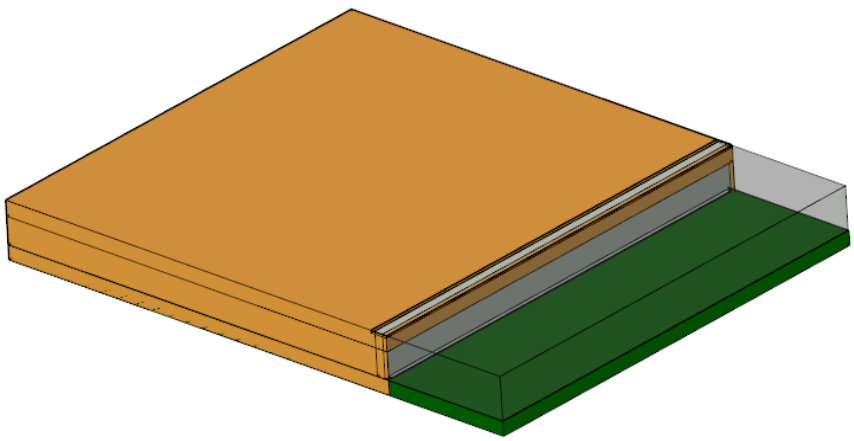

Figure 1.1: The SiP module with the metal shielding

2. Background Chapter 2

2.1. Antenna

An antenna is a metallic structure that can convert electrical signals into electromagnetic signals. It can also be used to receive electromagnetic signals and convert them into electrical signals [5].

The electrical signals are collected from the transmission line and converted into radio waves in the transmitting antenna, while the opposite happens in the receiving antenna. The radio waves from space are picked up by the receiving antenna, as illustrated in Figure 2.1, and converted into electrical signals and also given to the transmission line [6].

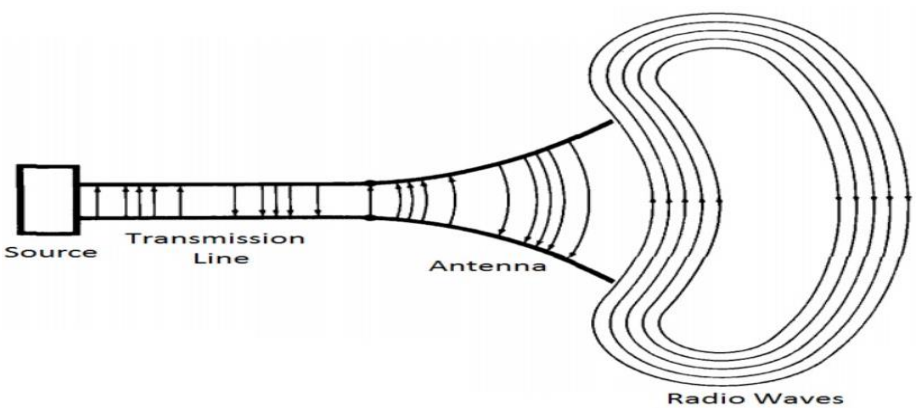

Figure 2.1: [6] An antenna connected to an AC source through the transmission line

2.2. Antenna Types

There are different types of antennas, each of which has its own specifications and performance. Some of the most commonly used are listed below [6].

2.2.1. Wire Antenna

Wire antennas include dipole antennas, short dipole antennas, monopole antennas and loop antennas. Wire antennas are used in vehicles, aircrafts, and buildings.

2.2.2. Microstrip Antenna

Microstrip antennas are another type of antenna that has become one of the most widely used antennas in various applications such as satellites, spacecraft, mobile phones. The rectangular microstrip patch antenna and the quarter-wave patch antenna can be referred to as the two types of microstrip antennas.

2.2.3. Aperture Antenna

These types of antennas have an opening in the surface through which electromagnetic waves are emitted. Slot antennas and horn antennas are most common types of aperture antennas.

2.3. Antenna Parameters

The behavior of antennas is judged by their parameters and some of the most important ones are listed below:

2.3.1. Antenna Polarization

Polarization is one of the most important parameters of the antenna and can be considered as a natural property of every antenna. The polarization of an antenna is the direction of the electric field generated by the antenna. In other words, the polarization determines the plane in which the fields of the transmitted signals change and is specified by the antenna designer. There are three different types of polarization: linear, circular and elliptical. Most antennas have linear polarization. With linear polarization, the change in polarization only occurs along one axis.

2.3.2. Antenna Radiation Pattern

The radiation pattern demonstrates the strength of the antenna radiation in each direction and can be displayed in a 2D or 3D diagram. A 2D pattern gives this information in a selected two dimensional section such as XZ, YZ and XY planes. The 3D radiation pattern shows the radiation of the antenna in all three dimensions. The radiation pattern of the antenna is divided into three categories: directional, omnidirectional and isotropic. Isotropic antennas, radiates with the same intensity in all directions and the radiation pattern is a shape of sphere. With omnidirectional antennas, the power is radiated uniformly in all directions in a particular plane and the radiation pattern looks like a ring, whereas directional antennas, radiate in a specific direction.

2.3.3. Antenna Gain and Directivity

The ratio of the maximum power density to the average radiated power density is defined as directivity and the gain is the measure of how much an antenna focuses the power received at its input port [7] and the function is shown in (1) [7]:

$$Gain = \eta.Dr \quad (1)$$

Directivity and gain are expressed in dB and dBi (decibels in relation to an isotropic radiator) respectively.

2.3.4. Antenna Radiation Efficiency

The radiation efficiency of an antenna indicates how effectively the antenna radiates into the space. The radiation efficiency indicates what proportion of the energy of the radio frequency (RF) signal can be radiated into the space by the antenna. In practice, the radiated power of the antenna is lower than the input power due to conduction losses, dielectric losses and reflection losses.

2.3.5. Antenna Bandwidth

The antenna bandwidth is defined as the frequency range in which the performance of the antenna corresponds to a certain standard characteristic. It is worth noting that antennas can be single-band, dual-band or multiple-band antennas in terms of the number of bandwidths they can cover.

2.3.6. Antenna Quality Factor

The losses of the antenna can be represented by the quality factor of the antenna. The quality factor, efficiency, gain and bandwidth can be considered as the figure of merit for the antenna, that are related to each other, and there is no complete freedom to optimize each of these elements independently [7]. Various losses such as radiation, ohmic, dielectric and surface losses, can affect the total quality factor, as the function is shown in (2) [8]:

$$\frac{1}{Qt} = \frac{1}{Qr} + \frac{1}{Qc} + \frac{1}{Qd} + \frac{1}{Qsw} \quad (2)$$

The surface wave loss (Q_{SW}) is very low and negligible for thin substrates [9] [10]

2.3.7. Antenna Input Impedance and Reflection Coefficient

The input impedance of an antenna is defined as the impedance that an antenna offers at its input connection. By way of explanation, the input impedance is the ratio of the input voltage to the current at the input connection of the antenna.

The Function is shown in (3):

$$Z = R + JX \quad (3)$$

R is the real part of the input impedance and can be regarded as the input resistance of the antenna. X is the imaginary part and represents the reactance provided by the antenna, changes with frequency. It is worth mentioning that some

factors such as feeding point, feeding mechanism, and operating frequency can affect the input impedance of the antenna [11].

The input impedance of the antenna can be regarded as the load impedance for the transmission line, which has the characteristic impedance Z_0 and is connected to the antenna from one side and to the AC source from the other side . When the AC source generates the incident signals and there is an impedance mismatch, the signal will be reflected at the antenna. The Function is shown in (4):

$$\Gamma = \left| \frac{ZL - Z0}{ZL + Z0} \right| \quad (4)$$

Where Z_L is the load impedance which equals to the input impedance of the antenna and Z_0 is the characteristic impedance of the transmission line.

The impedance mismatch between the antenna and the transmission lines can lead to a voltage standing wave ratio (VSWR). In the event of an impedance mismatch, some part of the signal can be reflected back to the transmission line. The ratio between the minimum and maximum amplitude of the standing wave is defined as VSWR. The highest VSWR is expected when there is an open circuit (the antenna is not connected) or a short circuit in the transmission line. The VSWR can be considered as a function of the reflection coefficient and the function is shown in (5):

$$VSWR = \frac{1 + \Gamma}{1 - \Gamma} \quad (5)$$

3. Effective Parameters Chapter 3

3.1. The effects of PCB properties on Monopole Antenna

The properties of a printed circuit board such as substrate thickness, permittivity, and loss tangent can influence the behavior of antennas. The properties of the substrate are of great importance for a microstrip antenna that is designed to resonate in the fundamental mode [12]. Extensive studies have been conducted to investigate the effects of substrate thickness and relative permittivity on the antennas [13] [14] [15], some of which are listed below:

3.1.1. Substrate Thickness

The thickness of the substrate can significantly affect the performance of the antenna and should be taken into account when designing antennas. Some studies have been conducted to investigate the influence of the thickness of the substrate on performance of the antenna [16] [17]. A higher substrate thickness usually results in a wider bandwidth of the microstrip antenna and can also affect the resonant frequency so that an increase in the thickness of the substrate, can reduce the resonant frequency [18]. Increased substrate thickness can also have disadvantages as it can generate surface waves that lead to power degradation and affect radiation [18]. Substrates with high thickness and low dielectric constant can offer properties such as loosely bound fields for radiation, higher efficiency and wider bandwidth [12]. On the other hand, substrates with higher dielectric constants and low thickness are suitable for microwave circuits, as smaller element size can be a result of a substrates with higher dielectric constants [18], however, their higher losses can decrease their efficiency and have relatively lower bandwidth [19].

3.1.2. Substrate Permittivity (ε_r)

Substrate permittivity can be considered as another important property of the substrate that can influence the performance of the antenna. Substrates that have higher permittivity, can make it possible to use smaller patches with less length and width in the microstrip antennas [18] .In general, as the permittivity of the dielectric substrate decreases and the substrate thickness increases, the gain, efficiency, directivity, resonance frequency and bandwidth of the microstrip antenna increase [7]. Therefore, to increase the electrical parameters of the

microstrip antenna and the bandwidth, a dielectric substrate with lower permittivity and higher thickness is preferred.

3.1.3. Loss Tangent

The loss tangent is another decisive factor when it comes to the performance of microstrip antennas. A higher value of the loss tangent leads to more dielectric losses of the substrate, which increases the bandwidth of the microstrip antenna, while decreasing the efficiency and gain of the antenna [7]. The value of the loss tangent can also influence the input resonance resistance. An increase in the loss tangent leads to a lower input resonance resistance of the microstrip antenna [7].

3.2. The effect of the ground planes on the antenna

Ground plane can be considered an influential factor in the design of small antennas. The lower frequency limit of the antenna increases as the ground plane gets smaller, which leads to a lower bandwidth [20]. Furthermore, the distance between the ground plane and the stripline is a crucial factor for the impedance matching of the antenna. In addition to the size and shape of the ground plane, the orientation of the antenna in relation to the ground plane and its position in the ground plane can also be considered as influencing factors for the performance of the antenna [21]. As for the resonant frequency, the ground plane can have a significant influence on this when the size of the ground plane is smaller than a quarter of the operating wavelength [1].

4.1. Design Requirements

The desired antenna should be designed on a very small area on module with the size of 13.4 ×10.6 mm and should have acceptable performance for simulation as shown in Table 4.1 when the package is placed on the carrier board with the size of 50 × 30 mm.

The designed antenna, which has a size of 3 × 10 mm, is expected to meet the specification when placed in the center of the smaller side of the carrier board. The thickness of the module on which the antenna was designed is 0.4 mm and the thickness of the carrier board, on which the project is centered is 1.6 mm, which is the most commonly used type of thickness. It is worth mentioning that the performance of the antenna with a carrier board thickness of 0.4 mm was also investigated in both simulation and measurement of the prototype.

Table 4.1: Target data for simulation results

Antenna type	Monopole antenna
Frequency Band	5.150 – 5.850 GHz, 5.925 – 7.125 GHz
Return loss	< -4.5 dB (5.150 – 5.850 GHz), < -4 dB (5.925 – 7.125 GHz)
Efficiency	> 65% (5.150 – 5.850 GHz) , > 60% (5.925 – 7.125 GHz)
Peak Gain	1-3 dBi
Radiation Pattern	Omni-directional
Physical size	3 × 10 mm
Substrate Material	FR-4 , 2 mm total thickness, 4.4 relative permittivity

The antenna is to be constructed on an FR4 laminate with the permittivity of 4.4. As can be seen in the Figure 4.1, there is a metal shield, for reasons of

electromagnetic compatibility (EMC), whose proximity to the antenna can influence the behavior of the antenna.

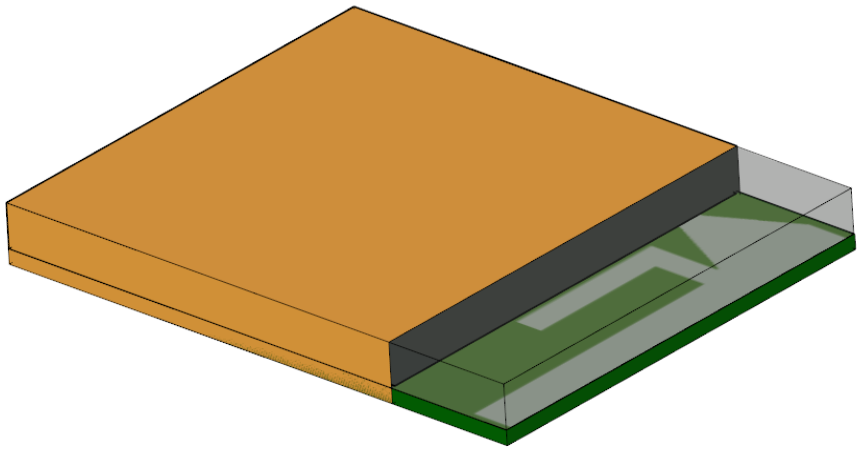

Figure 4.1: The designed antenna on the module

4.2. Printed Monopole Antenna

To begin the design, the first step should be to select the type of antenna according to the size and other expected specifications of the antenna. There are also other factors that can affect the behavior of the antenna that should be considered when designing the antenna, such as the feed structure, the ground plane, and the position of the antenna on the module, which are discussed in this paper. The printed monopole antenna was considered to be the right choice for Ultra Wide Band (UWB) applications due to its wide impedance bandwidth and the roughly omnidirectional radiation pattern in the azimuth plane [22].

There are different regularly shaped printed monopole antennas [22], including the printed rectangular monopole antenna (PRMA), the printed square monopole antenna (PSMA), the printed hexagonal monopole antenna (PHMA),

the printed triangular monopole antenna (PTMA), and other types, of which the printed rectangular monopole antenna was considered to be the proper choice for the design.

To calculate the lower band-edge frequency of the printed monopole antenna, the following formula can be used [22].

$$f_L = C/\lambda = 7.2/((L + r + p)) \text{ GHz} \quad (6)$$

The lower band-edge frequency can be calculated more properly by the equation bellow:

$$f_L = 7.2/((L + r + p) \times k) \text{ GHz} \quad (7)$$

For PSMA, S is the side length,

$$L = S, \quad r = \frac{S}{2\pi} \quad (8)$$

For PRMA, considering length = L and width = w,

$$L = L, \quad r = \frac{W}{2\pi} \quad (9)$$

P represents the length of the 50 Ω feed line and r is the effective radius of the equivalent cylindrical monopole antenna, both given in cm. To calculate the lower band-edge frequency within 10% , the factor k can be taken as an empirical value of 1.15 for FR4 substrate with $\mathcal{E}_r$ = 4.4 and a thickness of 1.59 mm, which is commonly used [22].

4.3. Feed Structure

The feed structure is the method of exciting the antenna through feed lines. The feeding mechanisms are divided into two types for microstrip antennas: the contacting and the non-contacting method. In the contacting method, the feed line is connected directly to the antenna to excite it. In the non-contacting method, the electromagnetic field for power transmission is applied between the microstrip line and the antenna.

Grounded Coplanar Waveguide (GCPWG) is the feeding structure that was chosen for the design. The online GCPWG calculator is shown in Figure 4.2. It is used to find the correct transmission line width to create a standard 50 Ω transmission line.

The Grounded Coplanar Waveguide, as presented in Figure 4.2 , consists of a layer on the substrate consisting of a signal line and a grounding layer on each side, and under the substrate there is a solid copper plane connected to the two grounding layers on the top of the substrate. The Grounded Coplanar Waveguide structure is used as feed structure for two reasons. First, because the top of the substrate of the SiP is covered by the ground and the antenna can be fed by a line surrounded by the ground plane at a distance of 0.5mm on each side by using GCPWG. The second reason is that the Grounded Coplanar Waveguide is easier to manufacture and can decrease radiation losses. In addition, components can be integrated directly on the transmission lines [21].

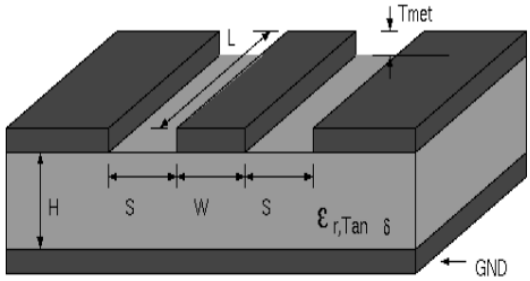

Metal width (W)	0.63	mm	calc
Metal spacing (S)	0.5	mm	calc
Trace length (L)	2.37	mm	
Metal thickness (Tmet)	0.035	mm	
Metal resistivity (RHO)	3e-08	Ohm - m	
Metal surface roughness (RGH)	0.001	mil -rms	
Substrate thickness (H)	0.33	mm	calc
Substrate relative dielectric constant (Er)	4.4		calc
Substrate loss tangent (tand)	0.02		
Frequency	7.125	GHz	
Analyze Reset	☑	Include bottom side ground	
Characteristic Impedance	49.9255	[ohms]	
Electrical Length	36.7431	[degrees]	

Figure 4.2: Grounded Coplanar waveguide calculator [23]

4.4. Transmission Line Impedance

In this design, the characteristic impedance of the transmission line (Z_0) is 50 Ω and to obtain this impedance, the Grounded Coplanar Waveguide calculator was used.

As shown in Figure 4.2, some parameters need to be considered to obtain the desired characteristic impedance in GCPWG, such as the metal spacing (S), the metal thickness (Tmet), the substrate thickness (H), the relative dielectric constant of the substrate (Er), the loss tangent of the substrate and other parameters. In this

design, the metal spacing is constant 0.5 mm based on the design specification, and the thickness of the ground layers for the bottom and top of the substrate is 0.035 mm and the thickness of the substrate is 0.33 mm . After entering all the design information, the metal width (W) calculated by the calculator was set to 0.63 mm to obtain a characteristic impedance of 50 Ω for the feedline.

The initial rectangular monopole antenna is shown in Figure 4.3 which consists of a rectangular part with a size of 2 × 2.53 mm and a feeding line connecting the excitation terminal (lumped port) to the antenna.

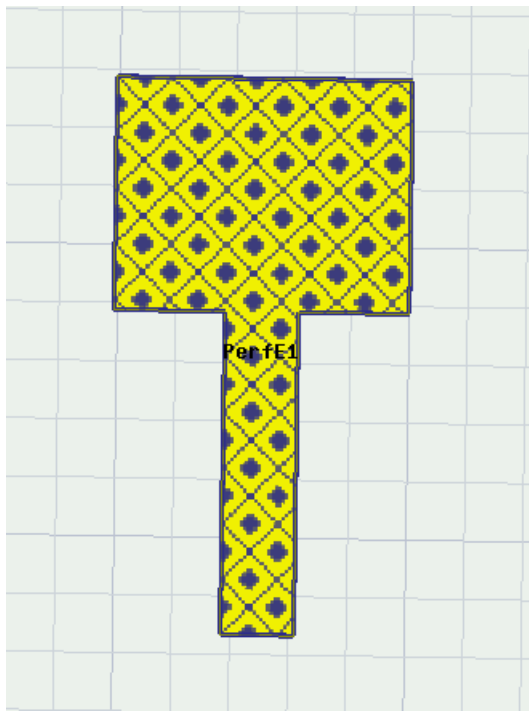

Figure 4.3: Basic monopole antenna model

As illustrated in Figure 4.4, the Scattering Coefficient (S11) parameter for the initial designed antenna on the module mounted on the carrier board with a size of 50 × 30 mm , is far away from the target area of the simulation.

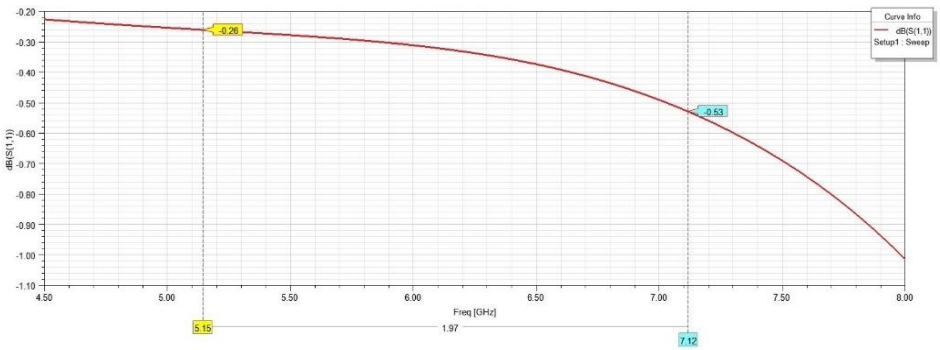

Figure 4.4: The initial antenna performance in HFSS

To improve the reflection coefficient, a resonance frequency is required in the frequency ranges from 5.150 GHz to 7.125 GHz. Therefore, the function (7) can be used to approximate the antenna size to achieve the desired resonant frequency. The antenna consists of two rectangular parts, where the larger part is 10 × 1 mm and the smaller part is 2 × 0.63 mm, connected to the feed line to excite the antenna. It is worth noting that, the width of the smaller rectangular part of the antenna is equal to the width of the feed line, which is 0.63 mm, as calculated in the grounded co-planar waveguide to obtain the characteristic impedance of 50 Ω for the transmission line. The same width is used for excitation port in High-Frequency Structure Simulator (HFSS).

The designed antenna is not fed from the center like a simple rectangular monopole antenna, as presented in Figure 4.5. The designed antenna is fed from the left side. As mentioned in the specification of the design, the total area for the design of the antenna is 3 × 10 mm and this small area makes the feeding structure a challenge. For this reason, the antenna was fed from the left side so that the current generated during excitation can flow across the entire width and length of the design to create a resonant frequency within the target frequency band. It is

worth noting that a slight change in the feeding point can make a big difference to the antenna's S11 parameter, which is particularly challenging designing small antennas. Figure 4.6 illustrates the reflection coefficient of the antenna.

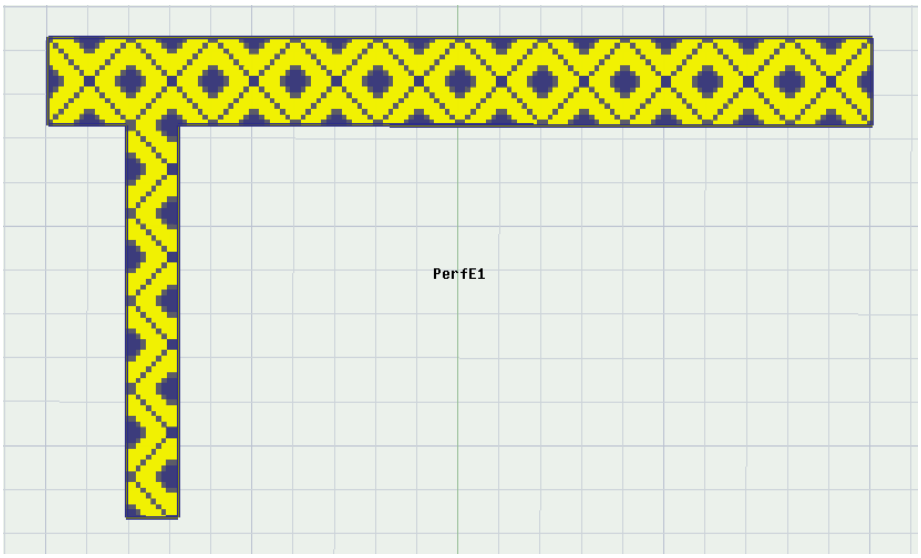

Figure 4.5: The antenna with proper size and feeding point

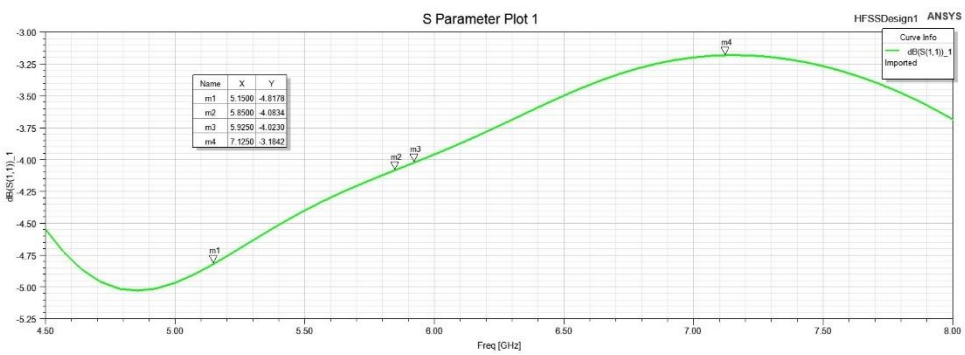

Figure 4.6: Simulation result for the antenna mounted on the module

4.5. Impedance Matching

4.5.1. Taper Structure

The matching of the load impedance (antenna) to the source impedance is called impedance matching of the antenna. For a better explanation, the impedance of the antenna(Z_L) must be matched to the characteristic impedance of the transmission line (Z_0) in order to transmit the maximum power. The advantages of impedance matching are the elimination of mismatch losses and the reduction of signal reflections at the load as well as the maximization of the power delivered to the antenna.

The difference between the width of the feeding line and the antenna can be considered as a sudden change that leads to a greater amount of reflections .Therefore, a tapered transition can be used to achieve better impedance matching by creating a smooth transition between the feedline and the antenna [21] , as presented in Figure 4.7

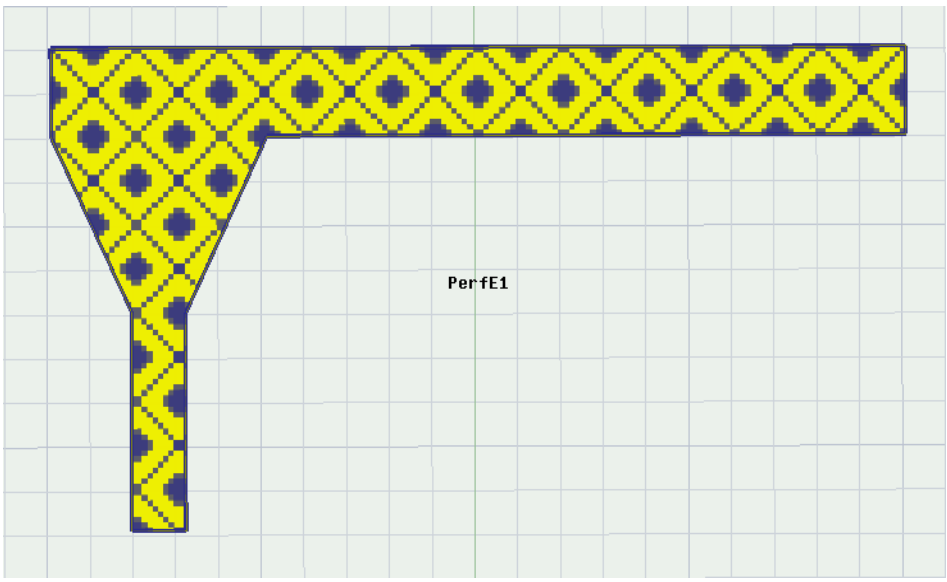

Figure 4.7: The designed antenna by adding taper structure

The reflection coefficient of the antenna, as shown in Figure 4.8, was improved by applying a taper structure with a maximum width of 0.95 mm and a length of 2 mm along the transmission line, on each side of the transmission line, resulting in better impedance matching.

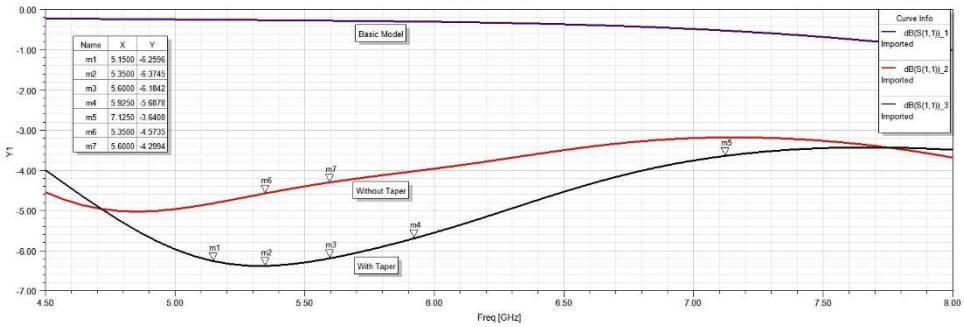

Figure 4.8: The comparison of results for S11 in HFSS

4.5.2. Adding L-shaped Part

To improve the reflection coefficient, an L-shaped part, as presented in Figure 4.9 was added to the design. The added part consists of two rectangles, one of which is 1.3 × 0.6 mm and the other is 0.6 × 4 mm, creating the L-shaped additional part.

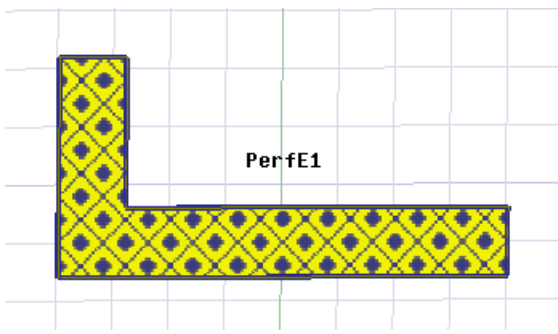

Figure 4.9: The L-shaped Part structure

The designed antenna after the addition of the L-shaped part is shown in Figure 4.10, which completes the model.

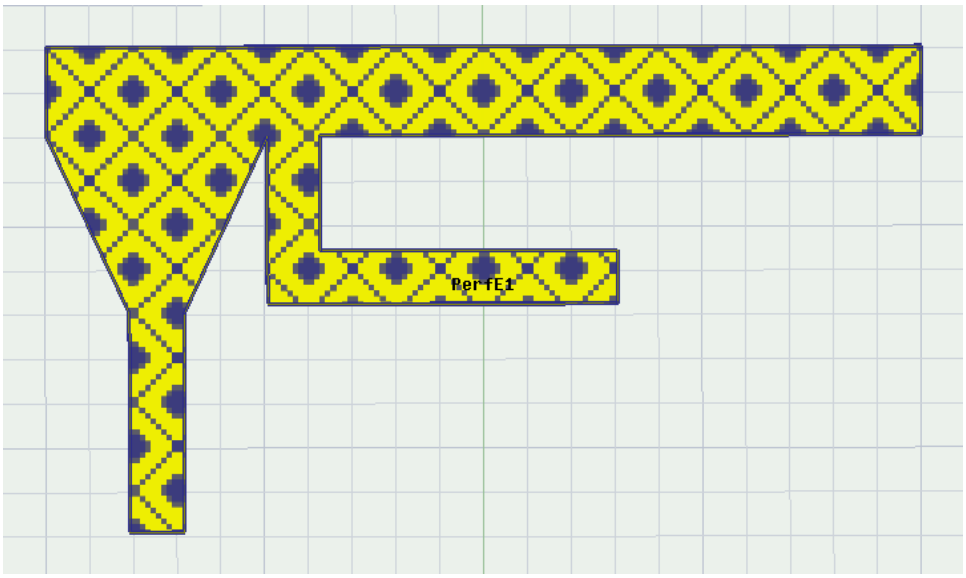

Figure 4.10: The complete antenna model after adding the L-shaped part

The added part had a positive influence on the designed antenna and resulted in a deeper S11 curve, as shown in Figure 4.11. In addition, the use of this L-shaped structure resulted in a resonant frequency at 6.1 GHz with an S11 value of -8.75 dB which means that the simulation result is within the range for the return loss. Figure 4.12 shows the radiation efficiency of the antenna.

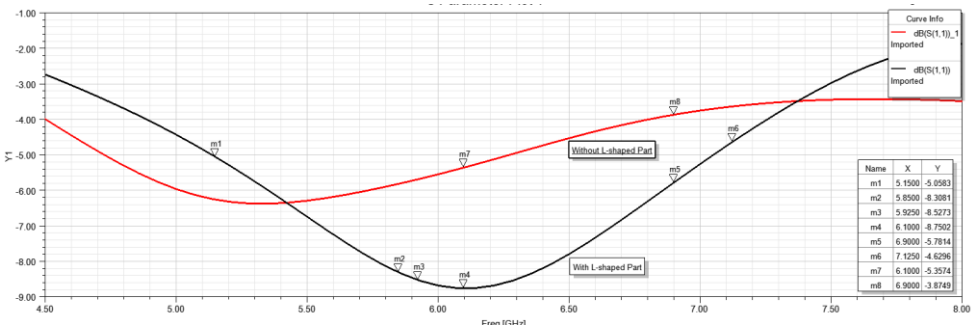

Figure 4.11: The comparison of S11 when adding the L-shaped part

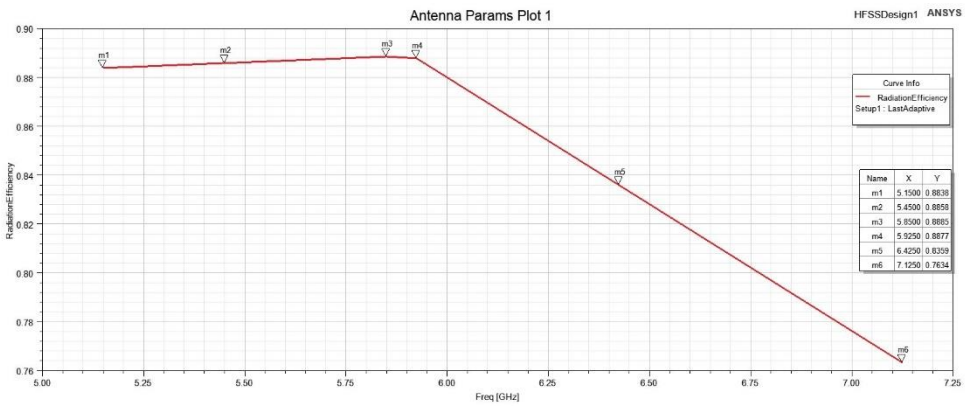

Figure 4.12: The simulation for radiation efficiency of the antenna in HFSS

4.6. Second Designed Antenna

As already mentioned, two antennas were designed in this project, with the focus on the designed antenna with the L-shaped part. The second designed antenna, as illustrated in Figure 4.13, also showed an almost acceptable performance with the targeted simulation specifications and the measurement of the prototype for the S11 parameter was also performed for it together with the first designed antenna.

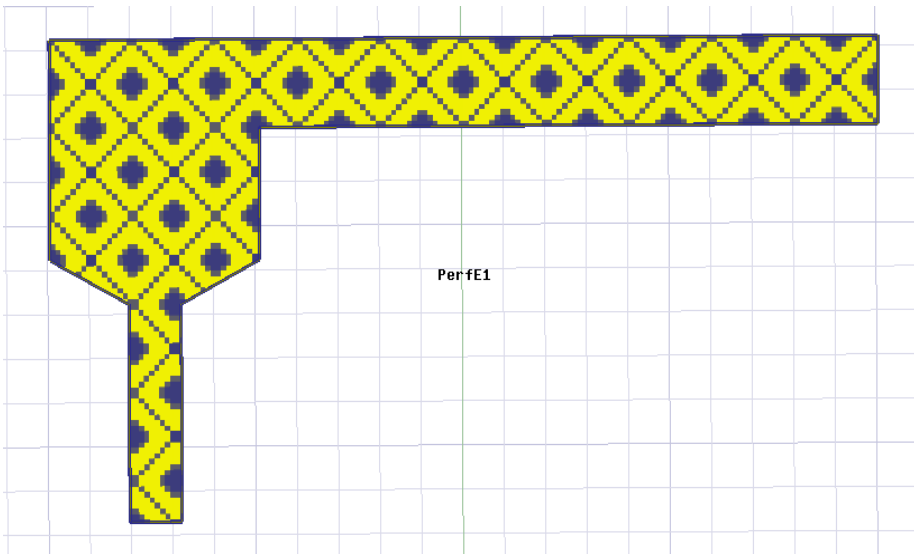

Figure 4.13: The second designed antenna with an additional rectangular part

The addition of a new rectangular section with a size of 2.53 × 1.5 mm made it possible to create a taper with a larger angle in connection with the transmission line. In other words, the maximum width of the tapper remained the same as the previously designed antenna, but the length of the tapper along the transmission line, was reduced from 2 mm to 0.5 mm, making the angle larger at the points close to the transmission line, resulting in a smoother transition and good impedance matching. As presented in Figures 4.14 and 4.15, a comparison was made between the reflection coefficient and radiation efficiency of this designed antenna and that of the designed main antenna performed.

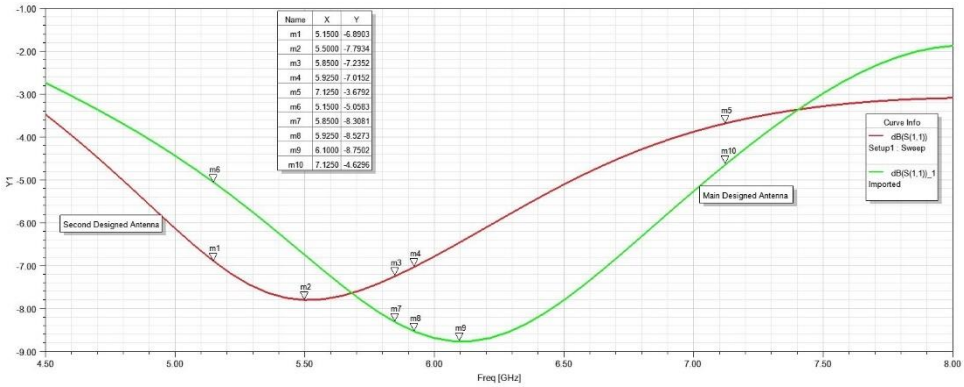

Figure 4.14: The comparison between the reflection coefficient of the two designed antennas

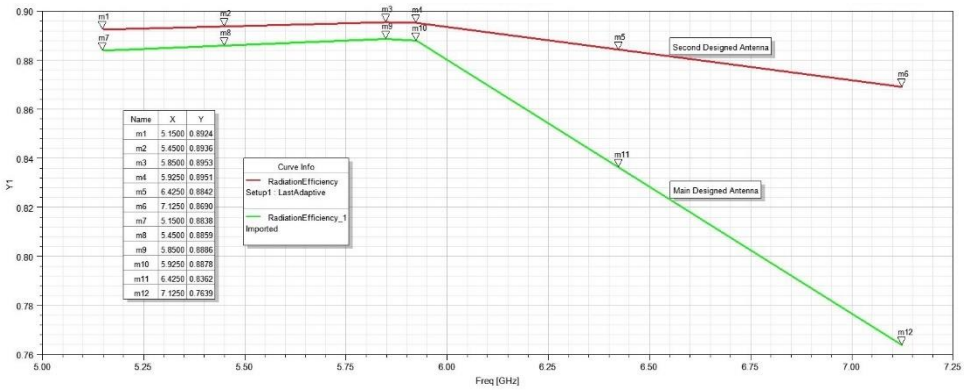

Figure 4.15: The comparison between the radiation efficiency of the two designed antennas

4.7. Antennas Performance with Different Positions of the Module on the Carrier Board

As mentioned in the project requirement, the antenna designed on the SiP should be attached to a carrier board. For better explanation, in practice, the customers of the SiP modules usually put this module on a larger printed circuit board(PCB) and the position of the SiP on the carrier board, can significantly affect the behavior of the designed antenna in terms of efficiency, gain, radiation pattern, return loss, and other practical parameters. For this reason, the most common options and their effects were investigated in this project. According to, the specification of the project, the SiP module should be placed on a 30 ×50 mm carrier board with a substrate of FR4 laminate with a permittivity of the 4.4 and a thickness of 1.6 mm, which is the most common thickness of carrier boards used by customers.

It is worth noting that the simulation results sought are for the case where the SiP is placed on the center edge of the smaller side of the carrier board (30 mm). This position is preferred by the company and the thesis focuses on this position, but the other two possibilities, such as placing the SiP on the right and left corner edges of the smaller side of the carrier board, were also investigated. As shown in Figure 4.16, the module with the main designed antenna is mounted on the left, center and right side of the carrier board in Ansys HFSS.

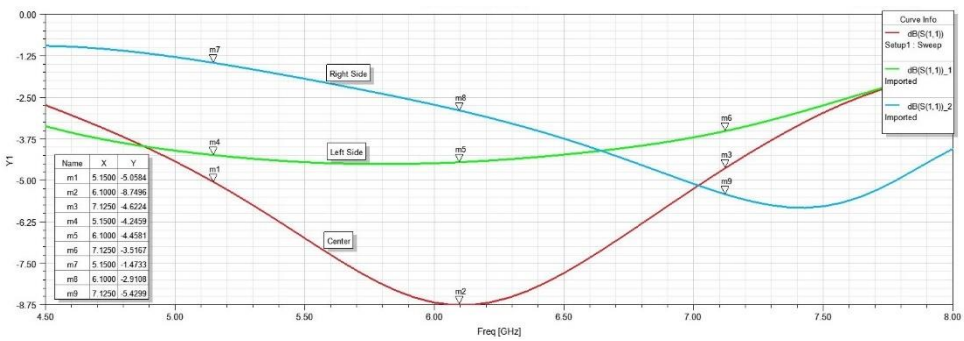

Figure 4.16: Comparison of S11 with different positions on the carrier board

As illustrated in Figure 4.16, the best return loss is achieved when the module is placed in the center of the narrower side of the carrier board, compared to placement in the left and right corners of the carrier board. When the module is placed at the left and right corners of the carrier board, the ground plane of the designed antenna is limited to the small ground plane of the SiP module at the left and right sides, respectively, which can affect the reflection coefficient of the designed antenna as shown in Figure 4.18. When the module is placed in the center of the narrower side of the carrier board, the parameter S11 is improved. The positive effect of this position on the radiation efficiency, as shown in Figure 4.17, is also considerable compared to two other positions of the module on the carrier board.

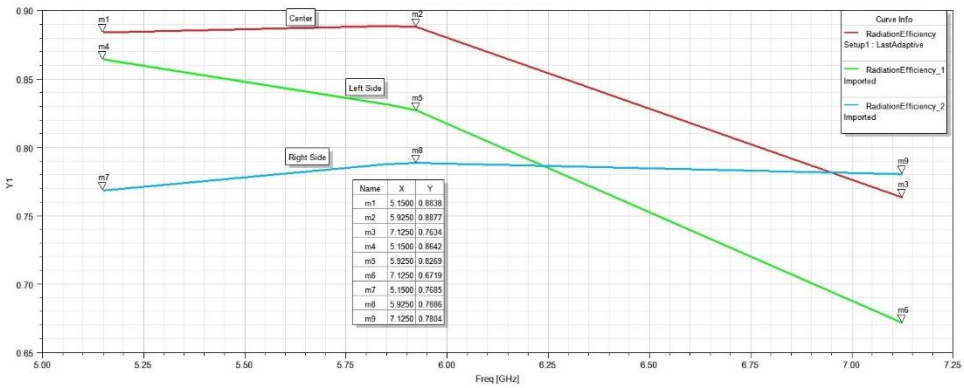

Figure 4.17: Comparison of the radiation efficiency of the design antenna with different positions on the carrier board

The effect of different positions of the module on the carrier board, as illustrated in Figure 4.18, is also considerable for the second designed antenna and the best performance for this model is also achieved when it is placed in the center of the narrower side of the carrier board.

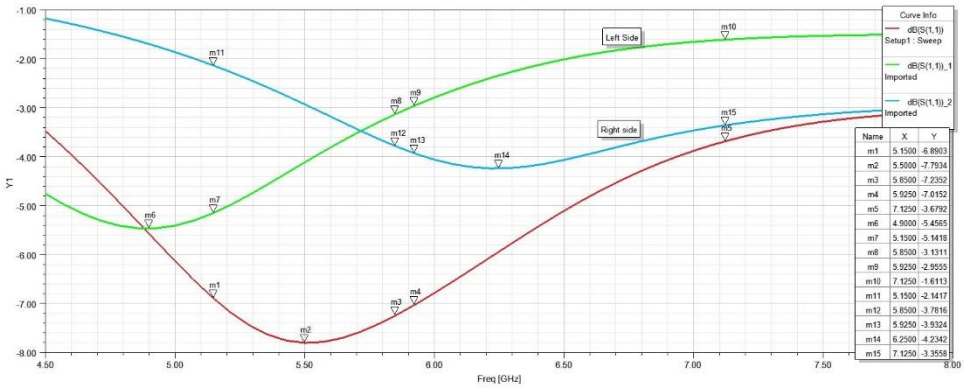

Figure 4.18: The S11 for the second designed antenna with different positions on the carrier board

4.8. Antenna Gain

The three-dimensional patterns of maximum gain of the antennas, shown in Figures 4.19 and 4.20, are compared at the frequency of 7.125 GHz, where the first designed antenna (with L-shaped part) is closer to the target gain for the simulation results.

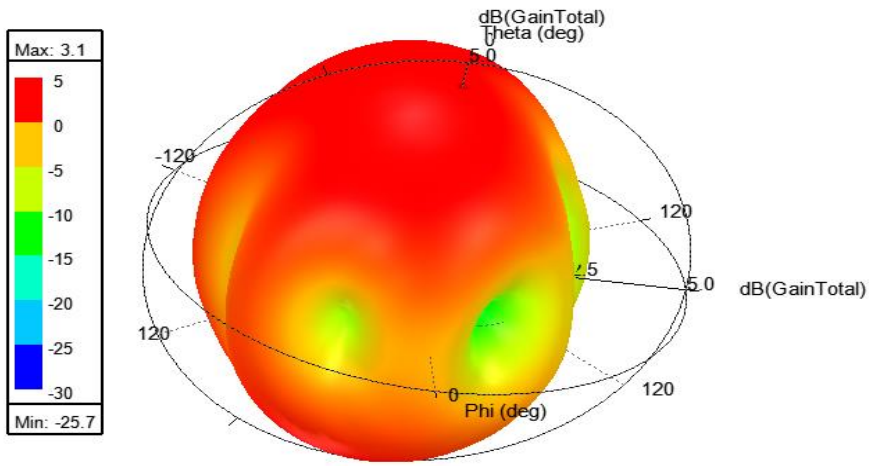

Figure 4.19: The 3D graph of the maximum gain for the designed antenna

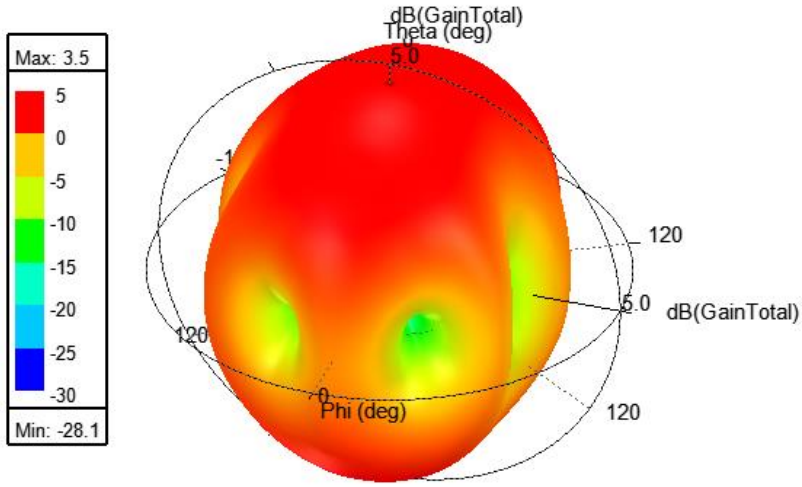

Figure 4.20: The 3D graph of the maximum gain of the second designed antenna

4.9. Antenna Three-dimensional Radiation Pattern

The designed antenna must have an omnidirectional radiation pattern. This means that a slot on the ground planes at least with the size of the antenna (3 × 10 mm) is required on the underside of the substrate of the module, where the antenna is located on the other side, and also on the ground planes on both sides of the carrier board in the area of the antenna. The size of the slot in the ground planes used in this design is 3.4 × 10.6 mm. As presented in Figure 4.21, the module is attached to the carrier board and the radiation pattern of the designed antenna is omnidirectional.

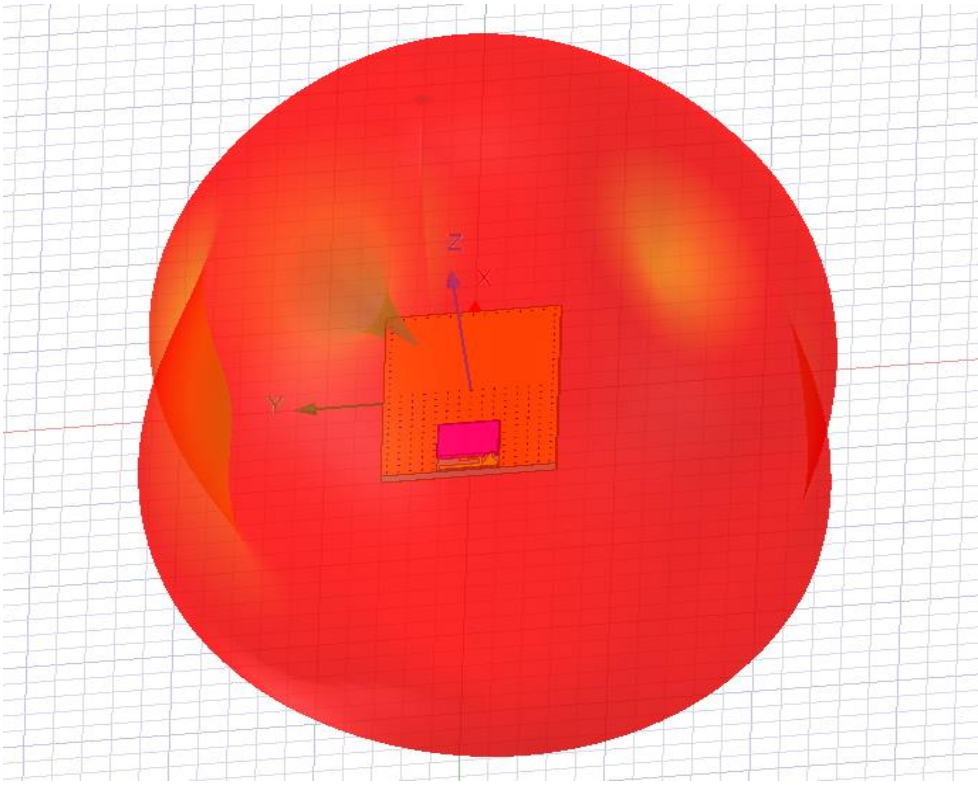

Figure 4.21: The 3D radiation pattern of the antenna with the module mounted on the carrier board at 5.925 GHz

The direction of the radiation pattern is important when designing the antenna. As illustrated in Figure 4.21, the direction of the radiation pattern should point to the outside of the edge of the carrier board on which the module is placed.

The three-dimensional radiation pattern from the side view, as shown in Figure 4.22, shows the omnidirectional radiation pattern.

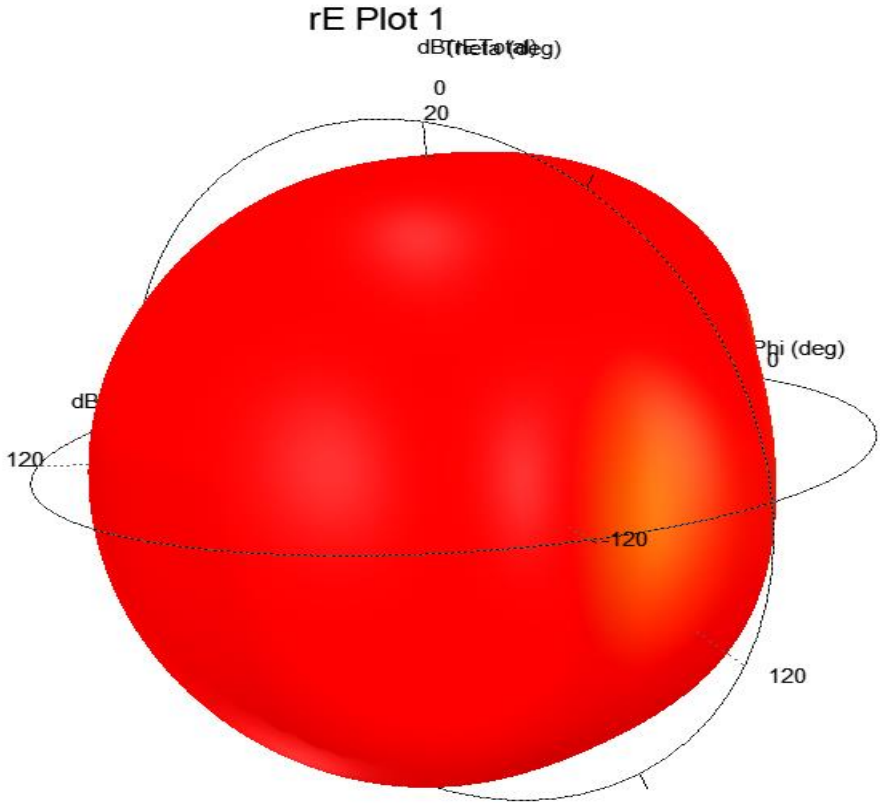

Figure 4.22: The 3D radiation pattern from the side view at 5.150GHz

4.10. The Behavior of the Antenna with Varying Thickness of the Carrier Board

The thickness of the carrier board on which the module is mounted is 1.6 mm for all simulation results, as this is the most common thickness. The behavior of the designed antenna with different thickness of the substrate of the carrier board was also investigated in this project. It is worth mentioning that the measurement of the antenna prototype was carried out with a substrate thickness of 0.4 mm for both the SiP module and the carrier board for cost reasons, as mentioned earlier. Therefore, the behavior of the antenna was also investigated with this substrate thickness of the carrier board. The reflection coefficient and radiation efficiency of the main designed antenna, are shown in Figures 4.23 and 4.24 for 1.6 and 0.4 mm thickness of the carrier board.

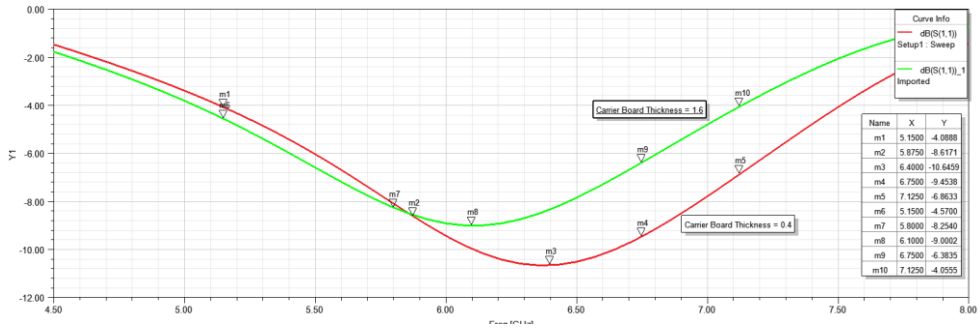

Figure 4.23: S11 for two different thicknesses of the carrier board in HFSS

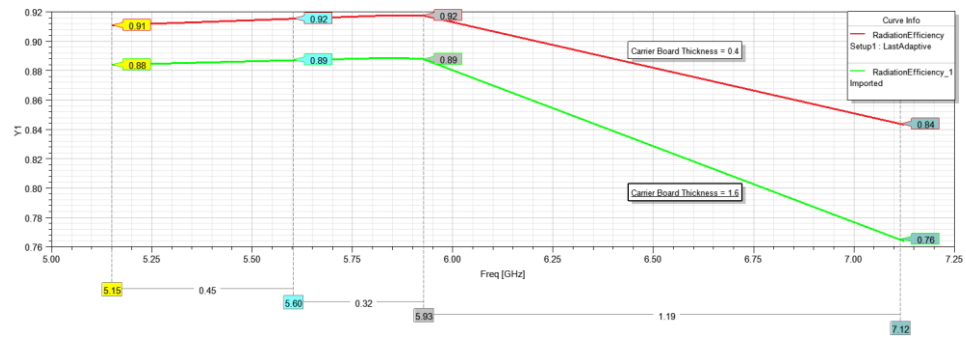

Figure 4.24: Radiation Efficiency for two different thicknesses of the carrier board

The effects of the different thickness of the carrier board for the second designed antenna are also shown in Figures 4.25 and 4.26.

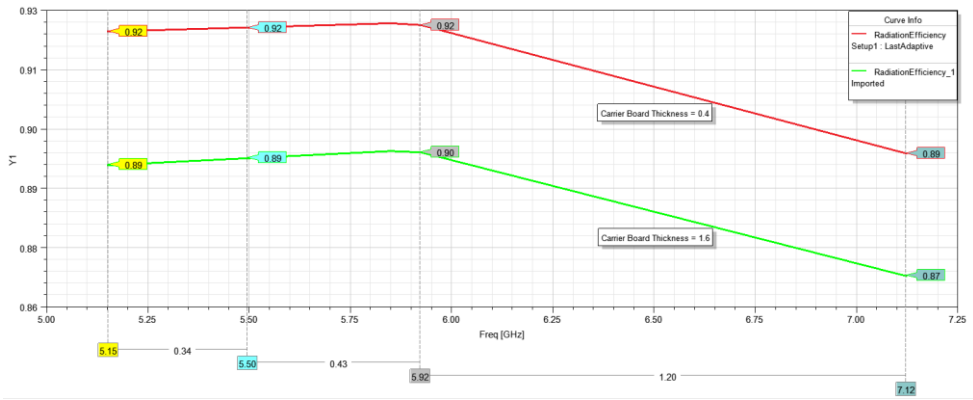

Figure 4.25: The effect of the two different thicknesses on the radiation efficiency of the second designed antenna

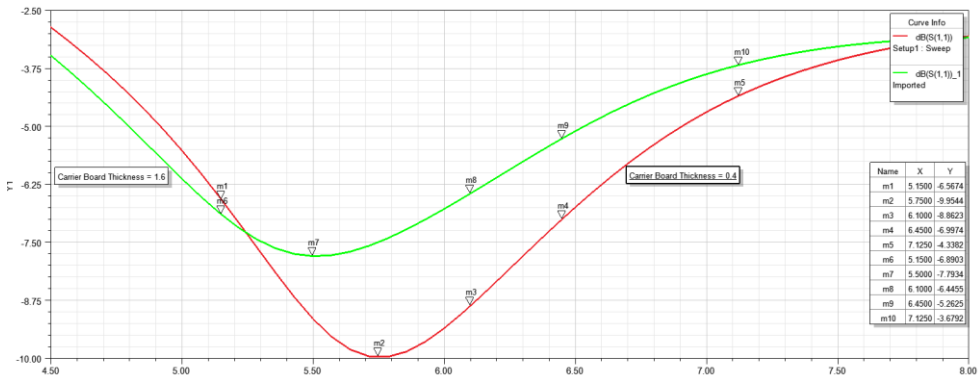

Figure 4.26: The influence of the thickness of the carrier board on S11 for the second designed antenna

4.11. The Effect of Antenna Length on the Resonant frequency

The designed antenna has a length of 10 mm and the effect of varying length was also investigated for the main designed antenna. In the designed model, as presented in Figure 4.27, the longer length of the antenna leads to a shift of the

resonant frequency to the lower frequency band and by decreasing the length of the designed antenna, the resonant frequency shifts to a higher frequency.

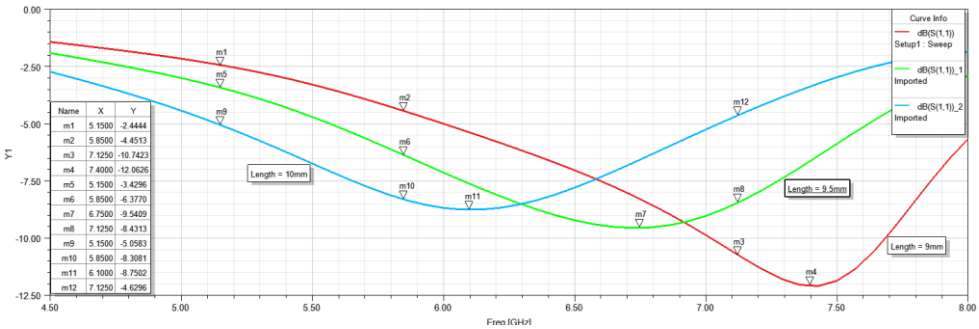

Figure 4.27: The effect of the different length of the antenna on S11

4.12. The Current Distribution and the Two-dimensional Radiation Pattern

The current distribution of the antenna, which is shown in Figures 4.28 and 4.29 for 5.15 GHz and 7.125 GHz, shows that the current is distributed approximately evenly over the antenna. It is worth noting that there may also be some power radiation from the ground plane near the antenna area. At 5.15 GHz, the ground plane around the feed line and also the ground plane on the carrier board on the left side of the antenna can radiate some power. The same happens when the antenna operates at 7.125 GHz, in which case there can also be some radiation from the ground plane of the carrier board on the right-hand side of the antenna.

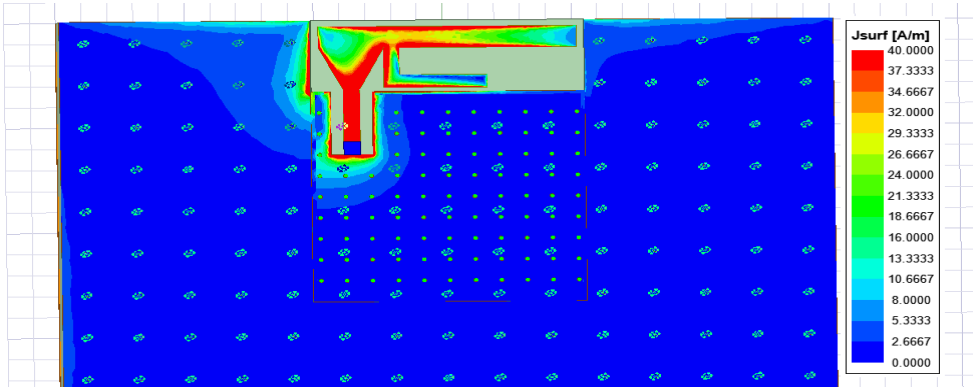

Figure 4.28: The current distribution of the antenna at 5.150 GHz

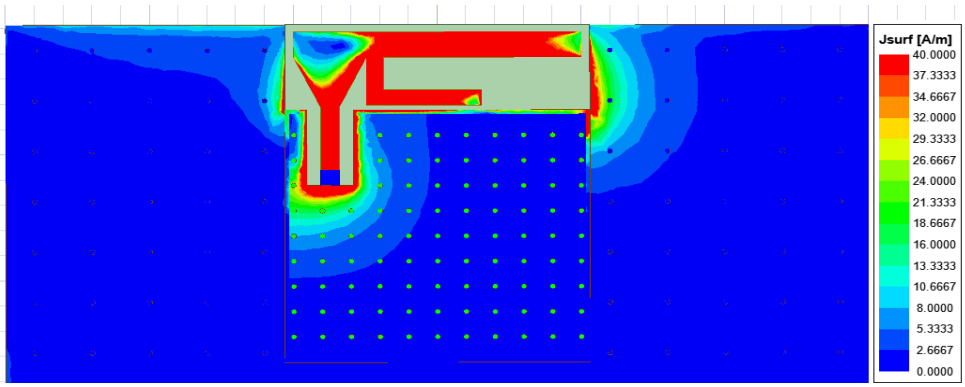

Figure 4.29: The current distribution of the antenna at 7.125 GHz

The same applies to the current distribution of the second designed antenna, which is shown in Figures 4.30 and 4.31. As can be seen in the figures, the ground planes can also be considered as part of the antenna as they can help to radiate the power. The current distribution in the design also shows that, at higher frequencies, for example 7.125 GHz, the current also tends to spread over the L-shaped part and across the length of the antenna which can make the radiation pattern of the antenna more directive towards the outer point of the carrier board where is module is mounted.

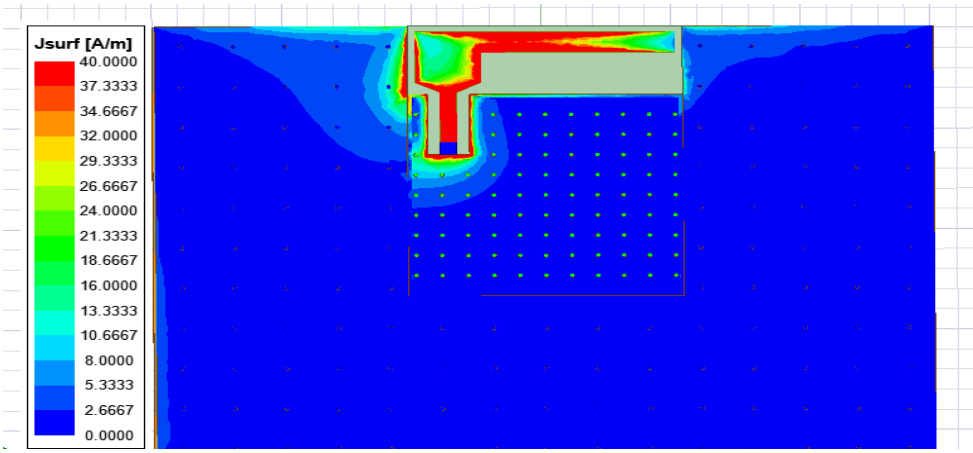

Figure 4.30: The current distribution for the second antenna at 5.150 GHz

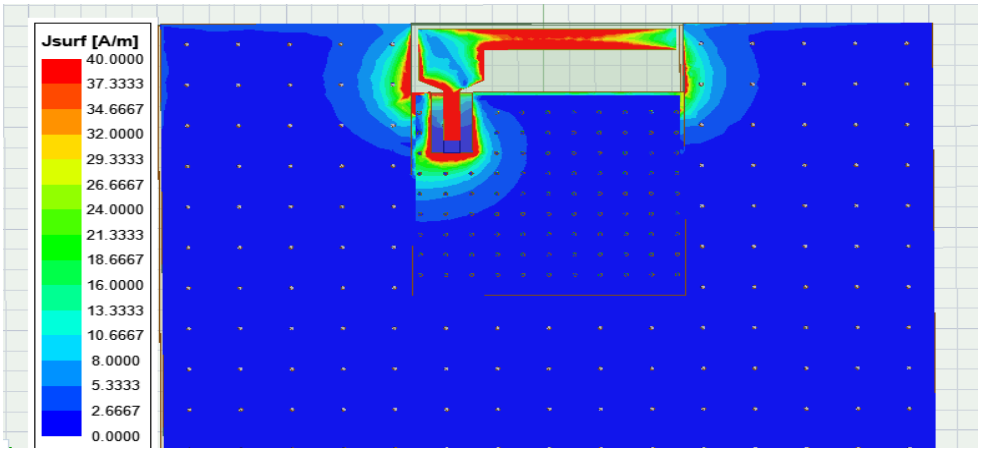

Figure 4.31: The current distribution of the second antenna at 7.125 GHz

The two dimensional radiation pattern for different frequencies in the elevation plane for the first antenna, is shown in Figures 4.32 and 4.33 and the Figures 4.34 and 4.35 also illustrate a better understanding of the radiation pattern in the XZ plane when the module is mounted on the carrier board.

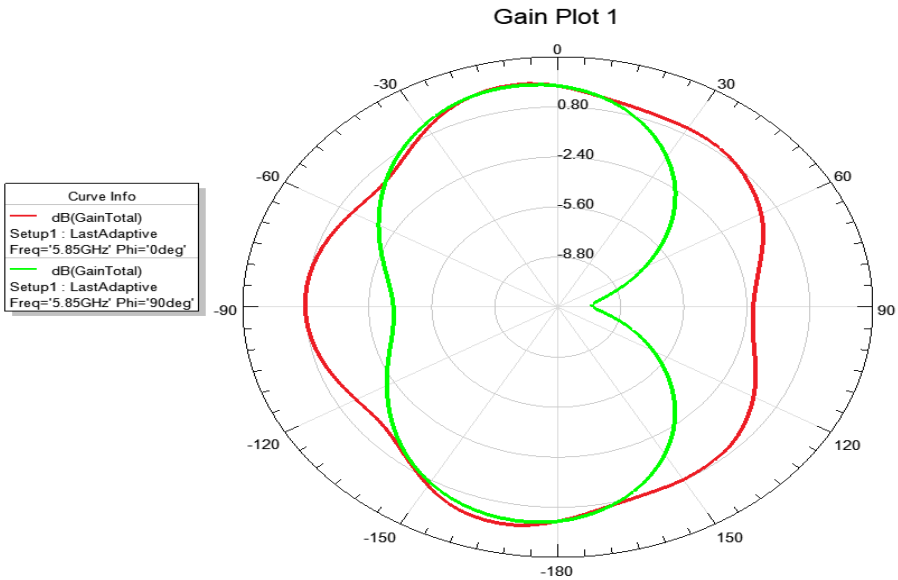

Figure 4.32: Radiation pattern in the elevation plane at 5.85GHz

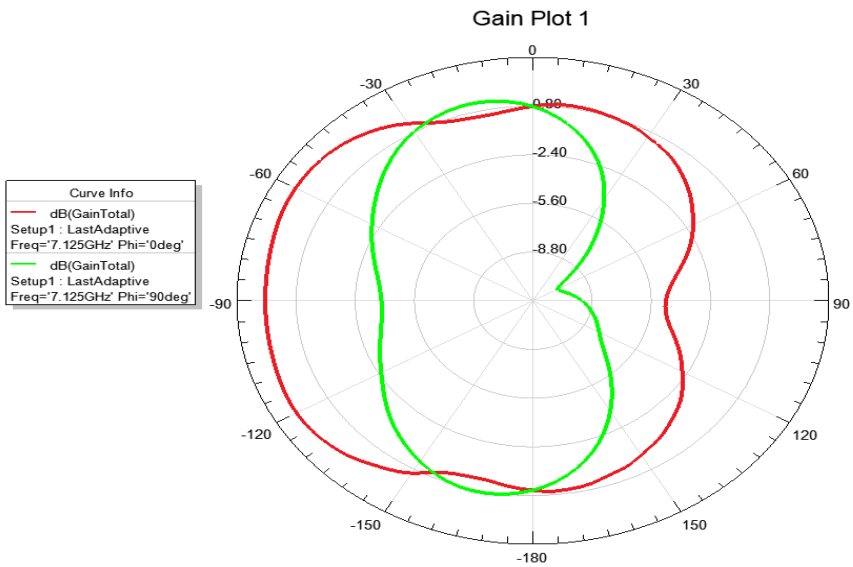

Figure 4.33: Radiation pattern in the elevation plane at 7.125 GHz

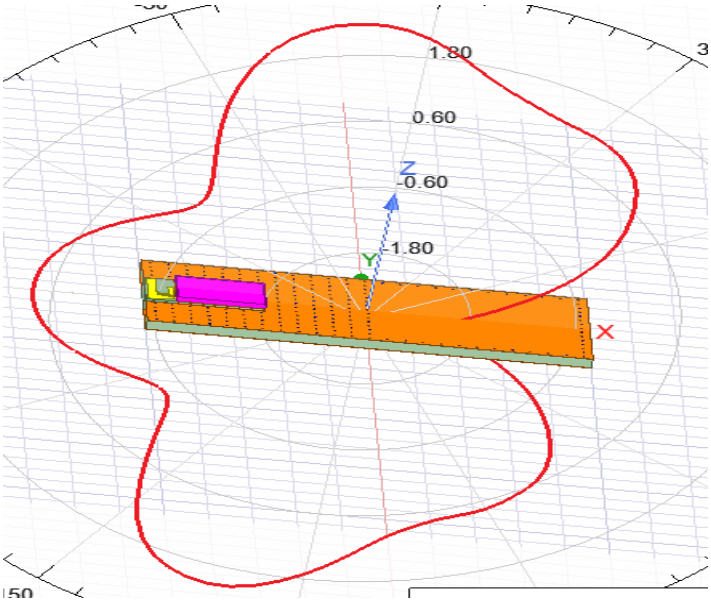

Figure 4.34: Two-dimensional radiation pattern in the XZ plane at 5.850 GHz

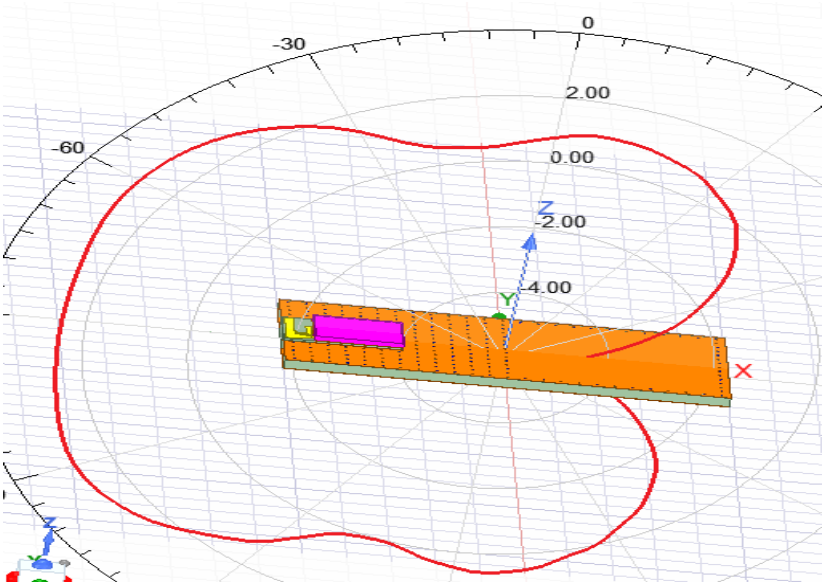

Figure 4.35: Two-dimensional radiation pattern in the XZ plane at 7.125 GHz

5.1. Drawing the Model in PCB Design Tool

For the antenna prototype measurements, Cadence Allegro was used to design the PCB to be sent for the manufacturing. The model of the two designed antennas and the carrier board, as shown in Figure 5.1, was implemented in the PCB tool. The FR4 substrate with relative permittivity of 4.4 and a thickness of 0.4 mm was used for both antennas and the carrier board.

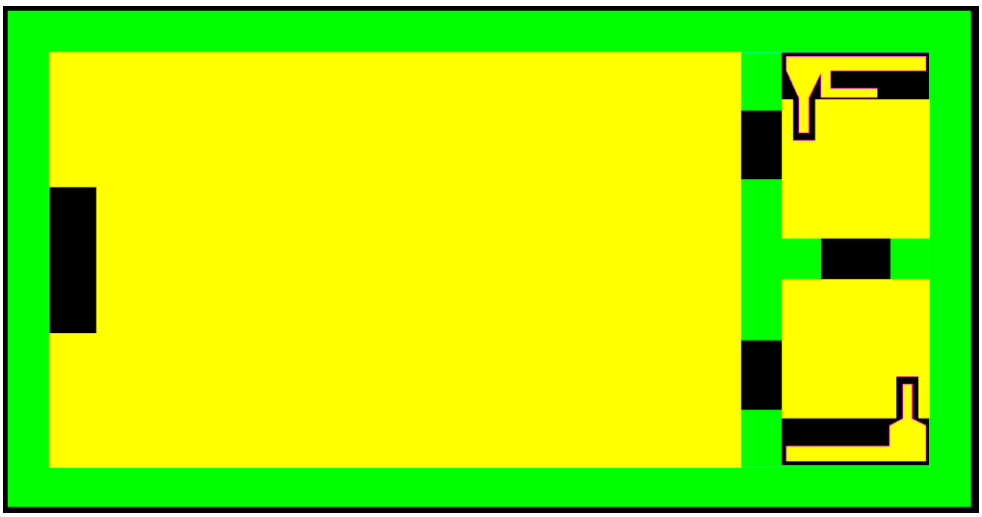

Figure 5.1: The antennas model and the carrier board in Cadence Allegro

The manufactured antenna and the carrier board, as presented in Figure 5.2, were separated from each other in the next step and the modules for the measurement were mounted on the carrier as shown in Figures 5.3 and 5.4.

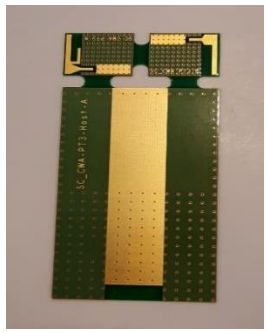

Figure 5.2: The two manufactured antennas and the carrier board

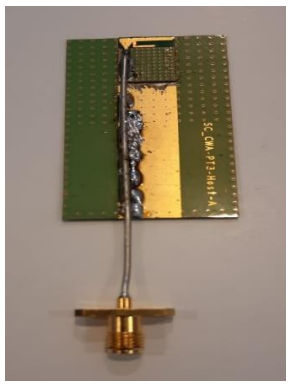

Figure 5.3: The first designed antenna mounted on the carrier board

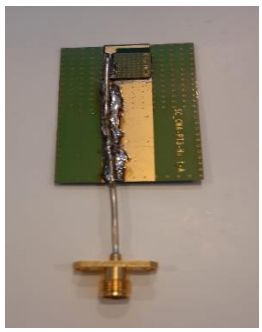

Figure 5.4: The second antenna mounted on the carrier board

5.2. Reflection Coefficient (S11)

The connectors were connected to the antenna, as shown in Figures 5.3 and 5.4, to apply the AC signal to the antenna. The inner wire of the connector was connected to the antenna in order to feed it and the outer part of the cable was connected to both the ground of the module and the carrier board by soldering. It can also provide stability to the cable during doing the measurements. In this method, the antennas, were fed from the top of the PCB. To perform the measurements ROHDE & SCHWARZ ZNB 20 Vector Network Analyzer and the anechoic chamber were used. The Vector Network Analyzer was calibrated before both the reflection coefficient test and the radiation pattern test. The test results of the measurements for parameter S11 for both antennas are shown in Figures 5.5 and 5.6. As illustrated in the Figure 5.5, there is a resonance at 6.140 GHz for the first antenna, which is very close to the corresponding resonance shown in the simulation at 6.1 GHz and the reflection coefficient is within the target range.

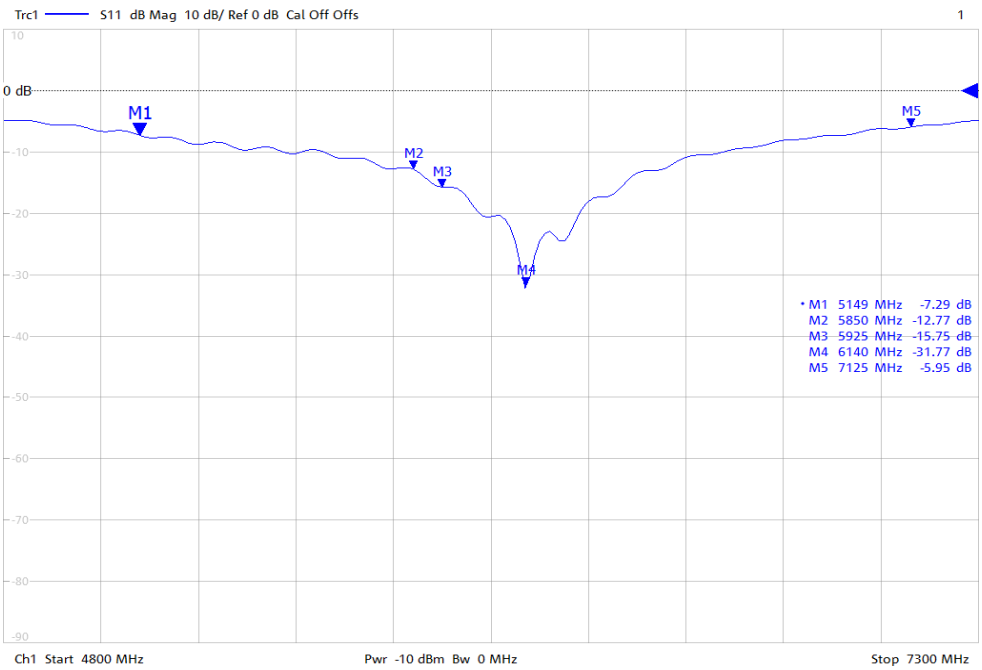

Figure 5.5: The measurement result of the S11 parameter of the first antenna

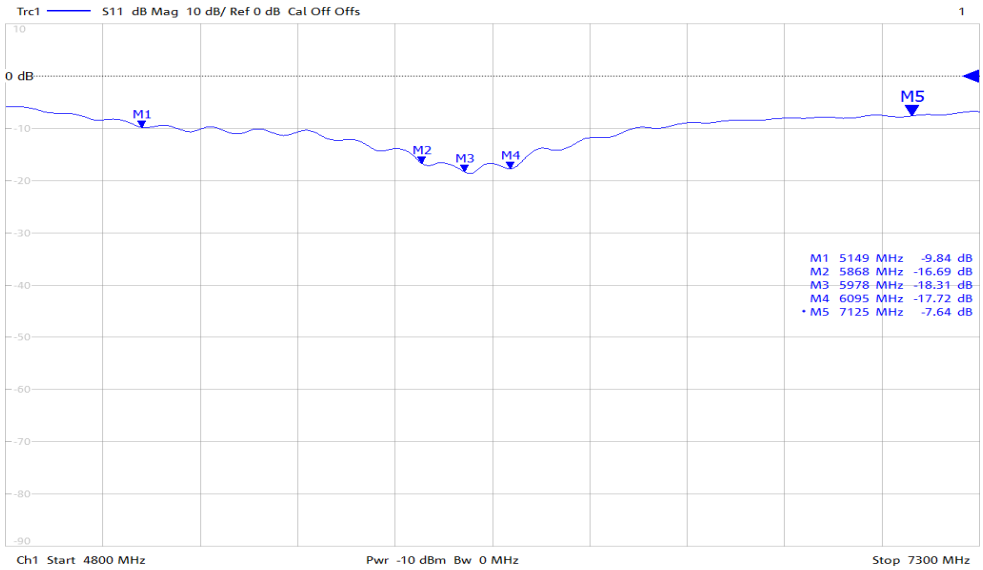

Figure 5.6: The measurement result of the S11 parameter for the second antenna

For the second antenna, as illustrated in Figure 5.6, there are three resonances at about 5.9 GHz, 6 GHz and 6.1GHz which also keeps the value of the reflection coefficient within the target range. The overall performance of the two antennas was acceptable in terms of S11 parameter in the target frequency band. Figure 5.7 shows the S11 parameter for the first antenna when covered by the plastic.

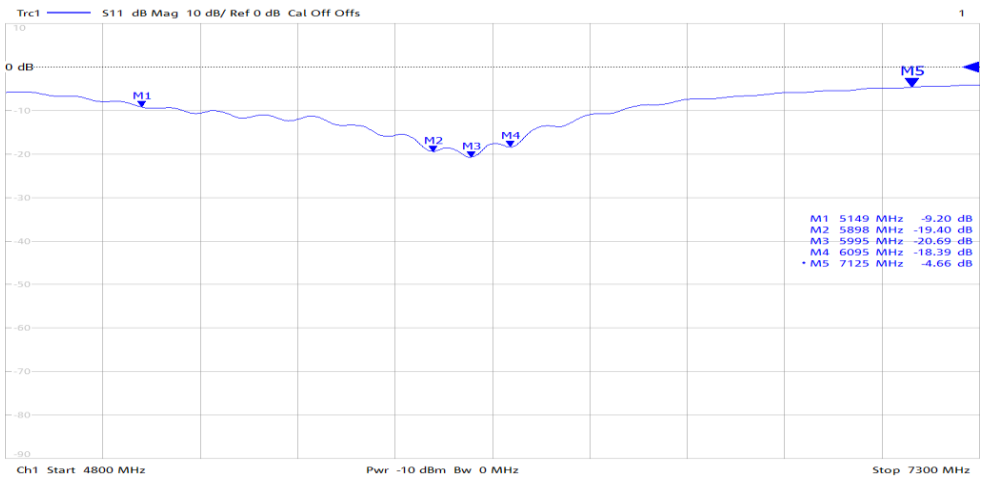

Figure 5.7: The measurement results of S11 for the first antenna covered by the plastic.

5.3. Radiation Pattern and Gain

To test the radiation pattern, the Vector Network Analyzer was calibrated again, this time with two ports, and connected to the anechoic chamber. Inside the chamber there is an antenna attached to the top of the chamber, shown in figure 5.8. For the radiation test, the designed antenna was placed in the center of the chamber at a fix distance from the chamber's antenna. The fixed antenna in the chamber and the designed antenna, acted as transmitter and receiver for different angles in the azimuth and elevation planes in this test. As a result, the S12 were measured for different angles, with values are very close to each other at some angles and far apart at some other angles. As this is not a precise method for measuring the radiation pattern of the antenna, it is not possible to make an accurate statement about the radiation pattern of the antenna using this method.

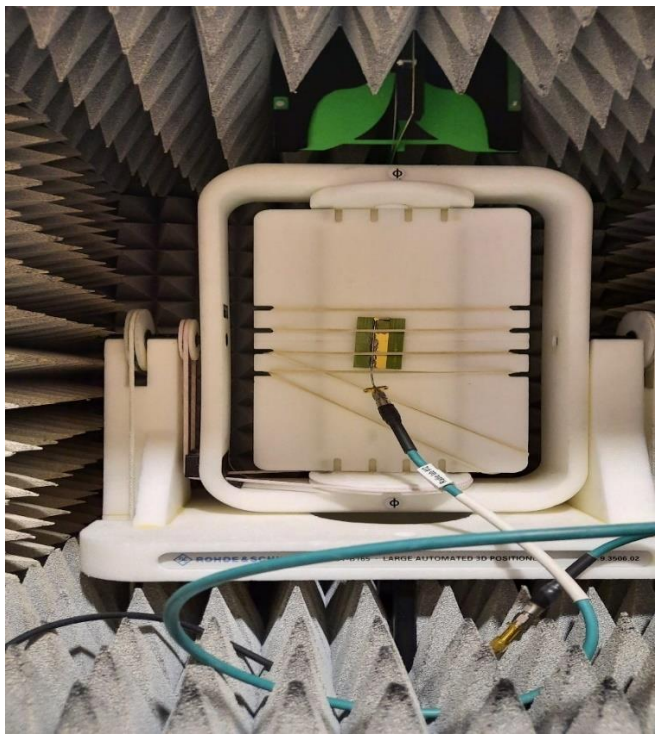

Figure 5.8: The antenna of the chamber (green antenna at the top) and the designed antenna in the center of the chamber

To calculate the gain of the main designed antenna, another test was performed using a horn antenna with the model of the ETS 3115 antenna. In this method, the designed antenna and the horn antenna were placed at a distance of 1 meter from each other ,as shown in Figure 5.9. The Vector Network Analyzer was first calibrated and then one port was connected to the designed antenna and the second port was connected to the horn antenna. The aim of this test was to measure the S21 results.

Figure 5.9: Measurement of the designed antenna gain using a horn antenna and Vector Network Analyzer

Figure 5.10 illustrates the S21 parameter from the Vector Network Analyzer. It is worth noting that there is no difference in the calculated gain values if we measure S12 instead of the parameter S21.

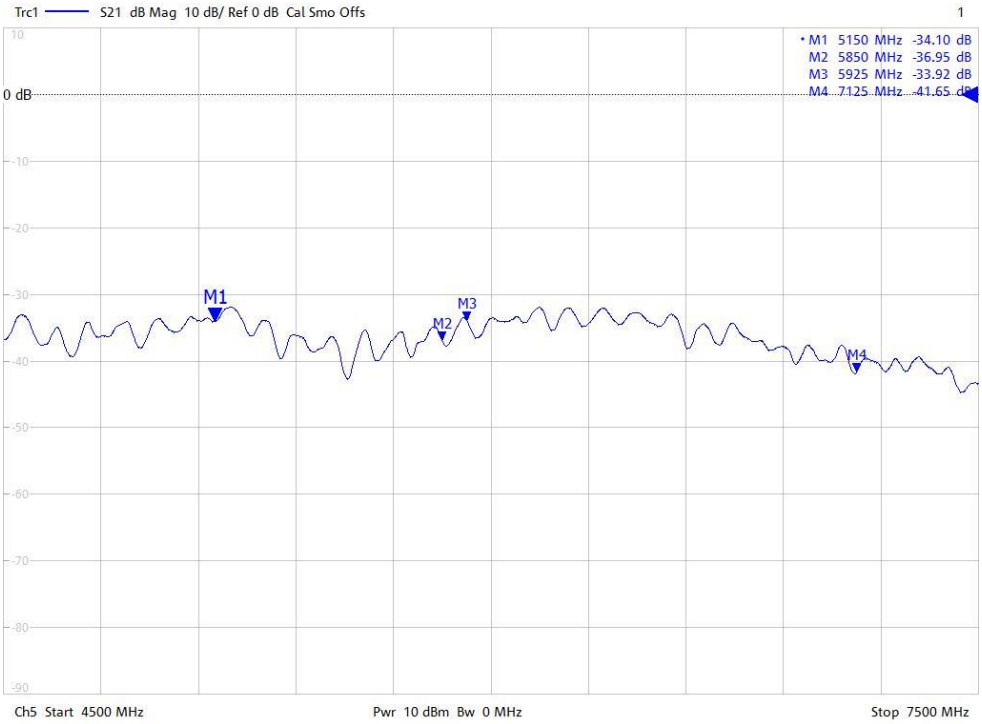

Figure 5.10: The S21 parameter for the measurement of the gain

In the next step, the Friss transmission equation, shown in (10) was used to calculate the gain of the designed antenna which is shown below:

$$G_r = P_r - P_t - G_t - 20\log\left(\frac{\lambda}{4\pi d}\right) \quad (10)$$

Where P_r and P_t represents the power of receiving and transmitting antenna respectively and G_t is the gain of the transmitting antenna, which was entered into the equation based on the horn antenna data sheet as a function of the frequency.

G_r represents the gain of the designed antenna calculated by the equation. λ and d are the wavelength and the distance between the two antennas respectively.

Table 5.1 shows the comparison between the calculated gain when measuring the prototype and the simulation results.

Table 5.1: The comparison between the simulation and the measurement results of the main designed antenna gain

Frequency (GHz)	5.150	5.850	5.925	6.900	7.125
Transmitting antenna gain (dBi)	10.6	9.5	9.5	9.4	9.4
S21 (dB)	-34.1	-36.95	-33.92	-37.5	-41.65
Maximum gain (measurement (dBi))	2	1.34	4.5	2.3	-1.55
Maximum gain (Simulation (dBi))	2.72	2.5	2.5	3.4	3.1
Distance (m)	1	1	1	1	1

6. Conclusion

The main focus of this work was to create a simulation model of a module with a size of 10.6 × 13.4 mm with an embedded antenna of 3 × 10 mm size. The designed antenna was expected to meet the target data of the simulation when the module is mounted in the center of the smaller side of the carrier board covering the frequency band from 5.150 GHz to 7.125 GHz. As a result of the thesis project, two antennas were designed. The first antenna was able to meet the design requirements for parameters in the simulation such as radiation efficiency, return loss and radiation pattern. For lower frequencies (5.150 - 5.850 GHz), it was also able to meet the requirements for the simulation's target data for gain and for higher frequencies it was almost able to meet the gain targets. The second designed antenna was also able to almost fulfil the requirements of the simulation.

For the starting point of the design , the model of a rectangular monopole antenna was chosen and the rectangular models were combined to form the initial model of the design. In the next step, the appropriate feed structure was selected and the accurate feeding point and feeding size of the design were also calculated. In the next step, a taper structure was added to the design for better impedance matching and the most appropriate size was calculated. The L-shaped part was also added to the design to improve the reflection coefficient.

The two designed antennas showed an omnidirectional radiation pattern in the simulation. In terms of radiation efficiency both showed an efficiency of more than 65 percent in the simulation. The return loss of the first antenna was completely within the range of the target data for the simulation and the second antenna was almost able to meet the return loss requirements.

It is worth mentioning that the measurements of the antenna prototype were also carried out to verify the simulation results. The antenna models and the carrier board were implemented in Cadence Allegro to fabricate the antennas on the PCB. Three types of tests were performed in this phase of the work. The first test concerned the reflection coefficient (S11) parameter of the antenna, the second test concerned the radiation pattern and the third test was for the gain . Both antennas showed satisfactory results for the S11 test. The gain test was performed only for the first antenna which showed acceptable results in some frequencies of the target band. To cover the frequency of 2.45 GHz, the design area of 3 × 10 mm for the antenna is very small, because as the frequency decreases, the size of the antenna increases. Therefore, to cover the frequency of 2.45 GHz, a larger antenna should be designed and connected externally to the module.

The final result of this thesis is two small antennas with high performance, covering the frequency range from 5.150 to 7.125 GHz in the simulation, whose performance was tested in some parameters by the measurements of the prototype.

7. Future work

There are some measures can be taken to get a higher performance antenna. One of these measures is to use passive elements such as capacitors or inductors to create a tunable antenna model that can be used for different applications. Another measure is to decrease the impact of the position of the module on the carrier board so that there is more freedom in the placement of the module on the carrier board and acceptable performance can be achieved.

As a further action for the future work, the measurements of the prototype can be carried out with a shield on the module in order to achieve a result that is closer to the real application of the antenna.

References

[1] P. Gao, J. Li and W. Wang, "Study of Ground Plane Effects on Monopole Antenna Performance.," *Electronics,* vol. 12, no. 12, p. 2681, 2023.

[2] Y. Liu, L.-M. Si, M. Wei, P. Yan, P. Yang, H. Lu and C. Zheng et al., "Some recent developments of microstrip antenna," *International Journal of Antennas and Propagation,* vol. 2012, p. 10, 2012.

[3] A. T. Mobashsher and A. Abbosh, "Utilizing symmetry of planar ultra-wideband antennas for size reduction and enhanced performance," *Antennas and Propagation Magazine,* vol. 57, no. 2, pp. 153-166, 2015.

[4] R. Cicchetti, A. Faraone, D. Caratelli and M. Simeoni, "Wideband, multiband, tunable,and smart antenna systems for mobile and UWB wireless applications 2014," *International Journal of Antennas and Propagation,* vol. 2015, p. 3, 2015.

[5] A. Q. Khan, M. Riaz and A. Bilal, "Various types of antenna with respect to their applications," *International journal of multidisciplinary sciences and engineering,* vol. 7, no. 3, pp. 1-8, 2016.

[6] R. Teja, "ElectronicsHub," Available: https://www.electronicshub.org/types-of-antennas/., accessed 11 05 2024.

[7] J. W. Salman, M. M. Ameen and S. O. Hassan, "Effects of the Loss Tangent, Dielectric Substrate Permittivity and Thickness on the Performance of Circular Microstrip Antennas.," Journal of *Engineering and Sustainable Development,* vol. 10, no. 1, pp. 1-13, 2006.

[8] . C. A. Balanis, Antenna Theory Analysis and Design, John Wiley and Sons, 1997.

[9] A. K. Verma, "Analysis of Circular Microstrip Antenna on Thick Substrate," *Journal of Microwaves and Optoelectronics,* vol. 2, no. 5, pp. 30-38, 2002.

[10] R. Garg et al., Microstrip Antenna Design Handbook, London: Artech.House, 2001.

[11] M. Deshpande and M. Bailey, "Input impedance of microstrip antennas," *IEEE Transactions on antennas and propagation,* vol. 30, no. 4, pp. 645-650, 1982.

[12] C. A. Balanis, Antenna theory: analysis and design, John Wiley & Sons, 2005.

[13] D. H. Schaubert, D. M. Pozar and A. Adrian, "Effect of microstrip antenna substrate thickness and permittivity: comparison of theories with experiment ," *IEEE Transactions on Antennas and Propagation,* vol. 37, no. 6, pp. 677-682, 1989.

[14] V. Rathi, S. Rawat and H. S. Pokhariya, "Study the effect of substrate thickness and permittivity on patch antenna," *IEEE International Conference on Signal Processing, Communications and Computing (ICSPCC),* pp. 1-4, 2011.

[15] P. Katehi and N. Alexopoulos, "On the effect of substrate thickness and permittivity on printed circuit dipole properties," *IEEE Transactions on Antennas and Propagation,* vol. 31, no. 1, pp. 34-39, 1983.

[16] M. Davidovitz and Y. Lo, "Input impedance of a probe-fed circular microstrip antenna with thick substrate," *IEEE transactions on antennas and propagation,* vol. 34, no. 7, pp. 905-911, 1986.

[17] J. Dahele and K. Lee, "Effect of substrate thickness on the performance of a circular-disk microstrip antenna," *IEEE Transactions on Antennas and Propagation,* vol. 31, no. 2, pp. 358-360, 1983.

[18] R. G. Mishra, J. Jayasinghe, G. Chathuranga and R. Mishra, "Analysis of the relationship between substrate properties and patch dimensions in rectangular-shaped microstrip antennas.," *In Intelligent Communication,*

Control and Devices: Proceedings of ICICCD 2017, pp. 65-72, 2018.

[19] D. M. Pozar, "Microstrip antennas," *Proceedings of the IEEE,* vol. 80, no. 1, pp. 79-91, 1992.

[20] W. Zhen and L. Hongtao, "Effect Analysis of Ground Plane Size on A UWB Monopole Antenna," *Electron. Inf. Warf. Technol,* vol. 30, pp. 67-90, 2015.

[21] H. Abdelgadir, "Evaluation, Characterization, and Optimization Of Miniaturized Microstrip Antenna For Wi-Fi 6/6E Application.," 2022.

[22] K. P. Ray, "Design Aspects of Printed Monopole Antennas for Ultra-Wide Band Applications," *International journal of antennas and propagation,* 2008.

[23] "Coplanar Waveguide Analysis/Synthesis Calculator," SOURCEFORGE, [Online]. Available: https://wcalc.sourceforge.net/cgi-bin/coplanar.cgi. , accessed 12 03 2024

Printed by Tryckeriet i E-huset, Lund 2024

LUND
UNIVERSITY

Series of Master's theses
Department of Electrical and Information Technology
LU/LTH-EIT 2024-972
http://www.eit.lth.se